

Aligning Agents like Large Language Models

Adam Jelley^{1†} Yuhan Cao² Dave Bignell² Amos Storkey¹ Sam Devlin² Tabish Rashid²

Abstract

Training agents to act competently in complex 3D environments from high-dimensional visual information is challenging. Reinforcement learning is conventionally used to train such agents, but requires a carefully designed reward function, and is difficult to scale to obtain robust agents that generalize to new tasks. In contrast, Large Language Models (LLMs) demonstrate impressively general capabilities resulting from large-scale pre-training and post-training alignment, but struggle to act in complex environments. This position paper draws explicit analogies between decision-making agents and LLMs, and argues that agents should be trained like LLMs to achieve more general, robust, and aligned behaviors. We provide a proof-of-concept to demonstrate how the procedure for training LLMs can be used to train an agent in a 3D video game environment from pixels. We investigate the importance of each stage of the LLM training pipeline, while providing guidance and insights for successfully applying this approach to agents. Our paper provides an alternative perspective to contemporary LLM Agents on how recent progress in LLMs can be leveraged for decision-making agents, and we hope will illuminate a path towards developing more generally capable agents for video games and beyond. Project summary and videos: <https://adamjelley.github.io/aligning-agents-like-llms>.

1. Introduction

The optimal approach for training agents to act in complex 3D environments without well-defined reward functions is an open question. Many modern video games provide such environments, where the state space, action space, and time-horizons are large enough that reinforcement learning (RL) from scratch is usually infeasible. However, even if possible, the resulting agent would not generalize to new objectives

¹School of Informatics, University of Edinburgh, Edinburgh, United Kingdom ²Microsoft Research, Cambridge, United Kingdom. Correspondence to: Adam Jelley <adam.jelley@ed.ac.uk>.

[†]Work done during internship at Microsoft Research, Cambridge.

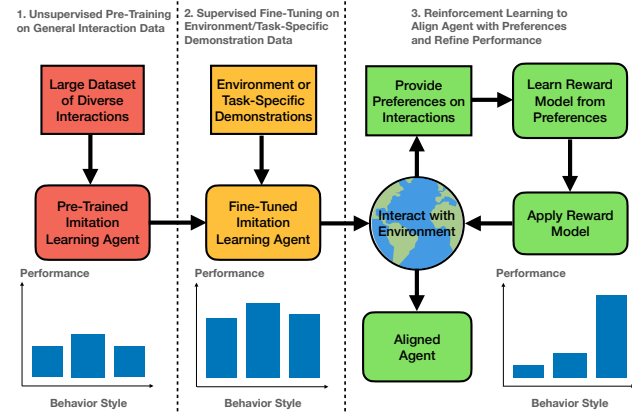


Figure 1. Illustration of our approach for training general agents in complex environments. Pre-training on a large, diverse dataset of interactions provides a base agent which can be more effectively fine-tuned with limited demonstrations. This agent can be further refined with RL, using a reward model or external reward function. This approach is analogous to the training of modern LLMs.

or environments. In contrast, large language models (LLMs) demonstrate impressively general capabilities resulting from large-scale pre-training, but struggle to act in complex low-level environments (Paglieri et al., 2024).

An analogous approach in the context of training agents is to leverage a large dataset of general human gameplay to pre-train an agent with imitation learning (IL). This provides an agent with a general understanding of player behavior, and there is evidence of generalization benefits from scaling up data and compute (Lee et al., 2022; Baker et al., 2022; Reed et al., 2022; Brohan et al., 2023; Pearce et al., 2024).

However, such an agent will inevitably learn to imitate all behaviors found within the human gameplay, including undesirable behaviors of novice or malicious players, analogous to unhelpful or toxic responses of unaligned LLMs (Ziegler et al., 2020). Additionally, game designers may want this general agent to perform a particular role, or act with a certain style or strategy (Aytemiz et al., 2021; Devlin et al., 2021). There is a parallel between making such an agent useful and aligning LLMs. In the same way that general LLM base models have been aligned for various purposes (Banerjee et al., 2023; Spatharioti et al., 2023; Chen et al., 2021b), we can imagine aligning a general decision-making agent with various objectives or environments.

This position paper argues that decision-making agents should be trained in the same manner as large language models (LLMs) to obtain analogous generality and robustness to objectives and environments. Specifically, agents should be trained and refined over multiple stages, typically involving: 1) *Unsupervised pre-training* on general behavior or gameplay data to obtain a general behavioral prior, 2) *Supervised fine-tuning* (SFT) on higher quality demonstration data of the relevant task or environment, 3) *Reinforcement learning* (RL), potentially from human feedback (RLHF), to refine and improve the behavior or further align the agent with implicit behavior preferences. To provide evidence for our position, we consider an academically illustrative part of a modern video game where the human behavior distribution is distinctly multi-modal, but we desire our agent to imitate a single mode of this distribution. This particular mode of behavior is difficult to learn from scratch with RL from pixels due to the size of the exploration space, and there are insufficient clean demonstrations of this mode for robust imitation learning. We demonstrate that this behavior mode can be reliably achieved by following the modern LLM training pipeline, and illustrate the importance of each stage. We train our agent from high-dimensional visual input with full game controller action output, maintaining the generality of our approach to other game environments, and demonstrating that the modern LLM training paradigm can be successfully applied to training agents in complex 3D environments. Our proof of concept provides evidence that many of the recent findings in the training of LLMs do indeed transfer to training agents, and could enable the training of more general and robust decision-making agents.

2. Context and Background

Large Scale Imitation Learning: Scaling up imitation learning and offline reinforcement learning (Levine et al., 2020) has recently gained popularity with the aim of demonstrating similar scaling laws to LLMs (Kaplan et al., 2020; Hoffmann et al., 2022) to obtain more general agents. For example, Decision Transformer (Chen et al., 2021a) proposed imitation learning with a transformer policy that can be conditioned on a desired return. Multi-Game Decision Transformers (Lee et al., 2022) extended this approach to learn multiple game policies, and GATO (Reed et al., 2022) demonstrated that a single model could learn hundreds of diverse tasks. RT1 (Brohan et al., 2022) shows similar scaling potential in robotics tasks, while RT2 (Brohan et al., 2023) integrated vision-language models and RoboCat (Bousmalis et al., 2023) demonstrated promising adaptation to new tasks. SIMA (SIMA-Team et al., 2024) incorporates language conditioning to enable generalization to new video games. Recently, Pearce et al. (2024) have confirmed the hypothesized scaling laws for imitation learning. While these approaches show the potential for scaling imitation learning, we argue

that these models are analogous to GPT-2 (Radford et al., 2018) in the rise of modern LLMs and that additional alignment stages can similarly be used to specialize and improve these models to make them as useful as modern LLMs.

Fine-tuning with Reinforcement Learning: The use of imitation learning as pre-training for reinforcement learning was first investigated to improve the sample efficiency of deep RL algorithms by reducing the exploration space (Hester et al., 2017; Vecerik et al., 2018). AlphaGo (Silver et al., 2016) and subsequently AlphaStar (Vinyals et al., 2019) demonstrated that large-scale imitation learning could provide a strong behavioral prior for environments like StarCraft where RL from scratch is infeasible. VPT (Baker et al., 2022) extended this paradigm to internet-scale Minecraft videos using an inverse dynamics model to enable imitation learning, before RL fine-tuning on task-specific rewards. While these works demonstrate the potential of fine-tuning large imitation models, they use hard-coded reward functions to maximize performance rather than align an agent’s behavior with new objectives or subjective preferences.

Reinforcement Learning from Human Feedback (RLHF): Training agents with human preferences has a long history, notably including Knox & Stone (2008) and Bennett et al. (2009), which has been reviewed by Wirth et al. (2017) and Zhang et al. (2021). The popular modern formulation of RLHF for deep learning was proposed by Christiano et al. (2017). This idea was extended by Ibarz et al. (2018) to include imitation learning as pre-training to improve the efficiency of reward modeling. PEBBLE (Lee et al., 2021) instead uses unsupervised pre-training to increase the diversity of initial behaviors. Abramson et al. (2022) and Milani et al. (2023) are closest to our position in using RLHF to refine the performance of large imitation agents in 3D simulated worlds, but do not make an explicit analogy or investigate the full LLM training pipeline.

Large Language and Vision Models: Radford et al. (2018) demonstrated that pre-training with an unsupervised generative task (next token prediction) on a large diverse corpus of text, followed by fine-tuning on a specific task, led to performance benefits compared to fine-tuning alone. Stiennon et al. (2020), following Ziegler et al. (2020), then popularized the use of RLHF to further fine-tune these models to align their responses with human preferences. This procedure led to InstructGPT (Ouyang et al., 2022), ChatGPT (OpenAI, 2022), and GPT-4 (OpenAI, 2023) as well as a wide range of other popular language models, such as Claude (Bai et al., 2022), Llama (Touvron et al., 2023) and Gemini (Gemini-Team et al., 2024). Generative pre-training has been shown to have equivalent benefits for vision tasks (Chen et al., 2020), and RLHF has similarly been used to refine image generation and vision-language models (VLMs) (Xu et al., 2023; Esser et al., 2024). More recently, RL with

pre-trained LLMs has been shown to improve reasoning capabilities in verifiable domains where external rewards can be defined (OpenAI et al., 2024; DeepSeek-AI et al., 2025). While components of the LLM training pipeline have been applied both individually and in combination to decision-making agents, in this paper we argue that the full pipeline (outlined in Appendix A) should be more widely and explicitly applied to agents to achieve similarly general agent models. We now turn to providing evidence to support this position with a concrete proof-of-concept.

3. Proof of Concept

3.1. Environment and Alignment Goal

As a proof of concept, we use the AAA video game Bleeding Edge¹, which was launched in 2020 for Xbox One². It is a team-based 4v4 online multi-player video game. The game is played with a third-person view, with the camera angle controlled by the player, so the environment is partially observable. Here, we focus on a single map, called Skygarden. This map is spread over three islands, including a main island and two launch islands (one for each team).

At the beginning of a game, players spawn at one of four points on their team’s launch island. From the spawn point, a player must navigate across the launch island to one of three jump pads that launch the player onto the main island. Depending on the jump pad selected, the player will be launched onto a different area of the main island, so players often take different jump pads. For the purpose of this work, we aim to train an agent to navigate across the launch island to a single one of the three jump pads. Since this navigation task requires around 10 seconds to complete for an optimal agent, without access to privileged information such as the agent location to shape a reward function, it would be extremely difficult to train an agent to complete this task with RL from visual input alone, as it would rarely leave the spawn area. On the other hand, an imitation learning agent will match the human distribution to reach all three of the jump pads. Therefore while the task is simple, it provides a clear motivation for alignment and a setting which we can quantitatively analyze to illustrate our position.

3.2. Implementation Details

Observation and Action Spaces: To maintain the generality of our approach to any 3D environment, we take visual gameplay observations $\mathbf{o}_t \in \mathbb{R}^{H \times W \times 3}$ as input, sampled at 10Hz. We do not provide any privileged information, so the agent only has access to visual information, as shown in Figure 2. The action space consists of 12 buttons and 2 joysticks. The left joystick controls movement, while the



Figure 2. Screenshots of the Ninja agent at a spawn point and heading towards the middle jump pad of the launch island.

right controls the camera angle. We decompose each joystick into an x and a y component which are independently discretized into 11 buckets to enable better modeling of multi-modal behavior distributions (compared to directly using continuous values), which is essential for our setting.

Dataset: For general pre-training, a dataset was extracted from recorded human gameplay, as described in Appendix B. This large unfiltered dataset consists of 71,940 individual player trajectories from 8788 matches recorded between 09-02-2020 and 10-19-2022, which amounts to 9875 hours (1.12 years) of individual gameplay. For the purposes of this work, we use a base agent that was trained for roughly one epoch on this dataset. Considering the success of recent foundation models, we note that given our unified observation and action spaces, it may be possible to instead train across games to obtain this base model, as explored in previous work (Reed et al., 2022; SIMA-Team et al., 2024).

Architecture and Training: For the policy, we use a GPT-2 (Radford et al., 2019) causal transformer architecture with 103M parameters, similar to that used by VPT (Baker et al., 2022). Observations from the human gameplay $\mathbf{o}_t \in \mathbb{R}^{H \times W \times 3}$ are taken directly as input to a convolutional encoder to give observation embeddings \mathbf{z}_t . The transformer is trained with a context window of $H = 32$ timesteps (around 3s of gameplay given the 10Hz sampling). The context window is important since the game is partially observable: longer context provides the agent with a more Markovian state, but at the cost of quadratic computational complexity. We note that developments in extending the context length of transformers, such as modified attention mechanisms (Beltagy et al., 2020), or even Retrieval-Augmented Generation (RAG) (Lewis et al., 2021), could also be investigated here to help address partial observability. The transformer and convolutional encoder are both trained end to end with a cross-entropy loss over all 16 discrete action components to provide a policy $\pi(a_t | o_t, a_{t-1} \dots o_{t-H})$. While we only consider prior observation and action context for simplicity in this proof-of-concept, text embeddings e corresponding to game or task instructions (likely to be an integral part of a general agent) could also be straightforwardly included as conditioning here, providing an instruction-conditioned policy $\pi(a_t | o_t, a_{t-1} \dots o_{t-H}; e_t)$ similar to SIMA (SIMA-Team et al., 2024). Full architecture and training details are provided in Appendix C.

¹ www.bleedingedge.com/en

² www.pcgamingwiki.com/wiki/Bleeding_Edge

Evaluation: To evaluate our models, we run each agent online in the game environment and record which jump pad is reached over 1000 episodes. To run an agent online, we initialized the *Ninja* character with an empty context buffer at one of the spawn points at random. We run the agent until it reaches one of the jump pads or times out.

3.3. Does large scale pre-training provide generalization benefits in the context of agents?

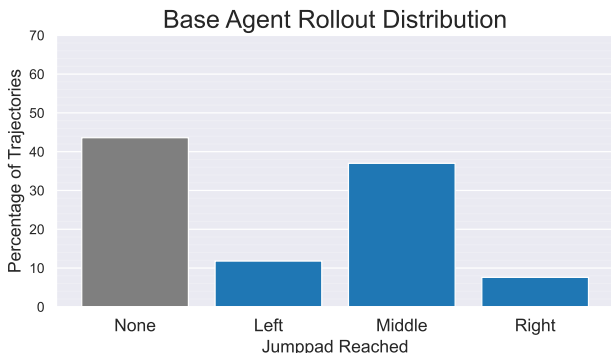


Figure 3. Distribution of jump pads reached by the base agent.

We begin by evaluating our base model, which achieves the jump pad distribution shown in Figure 3. We see that our agent fails to reach a jump pad 44% of the time, and has a bias towards the middle jump pad, reflecting human behavior. Our base model therefore provides a reasonable behavioral prior, and is much better than a randomly initialized agent (which has a 0% success rate). However, the success rate could be improved, which is partly due to distribution shift between the offline data and the online environment. For example, the base model was trained on data containing all thirteen possible characters, while our online evaluation only uses the default *Ninja* character. Additionally, we initialize our agents online at the spawn point with an empty context buffer, while in training the agent will have access to context including a spawn animation and prior gameplay. While measures can be taken to avoid distribution shift, offline-only learning is inherently challenging (Ostrovski et al., 2021) as discussed in Appendix D, demonstrating the need for some online behavior refinement (see Section 3.6).

Following the LLM pipeline, we now fine-tune our agent on a smaller curated dataset. We curated 300 successful trajectories (100 per jump pad) for fine-tuning, all of which involved the character *Ninja* and were filtered to contain only the first part of the trajectory until a jump pad was reached. We fine-tune until convergence as described in Appendix C. More generally, this stage could consist of fine-tuning on any smaller, high-quality demonstration data. We see in Figure 4 that the success rate of reaching a jump pad is now substantially higher (with only an 11% failure rate),

and that the agent more evenly reaches all three jump pads (corresponding to the balanced fine-tuning dataset).

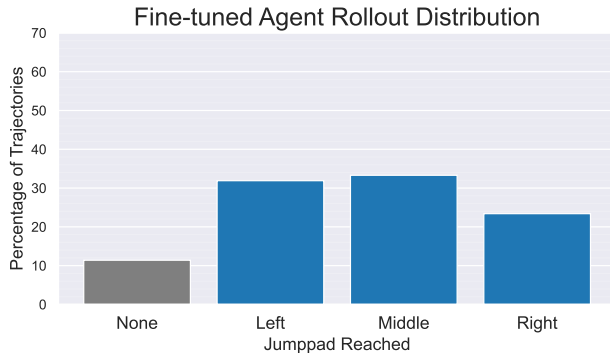


Figure 4. Distribution of jump pads reached by the base agent after supervised fine-tuning (SFT) on a task-specific dataset.

At this stage, it is natural to ask whether the general pre-training was beneficial or whether the model could have been trained from scratch on our task-relevant dataset directly. After all, if clean demonstrations of the desired behavior are available, why train the agent on messy, less-relevant data? To investigate this, we train an equivalent architecture model from scratch until convergence on the fine-tuning dataset only (see Appendix C for details). The evaluation of this model is shown below in Figure 5.

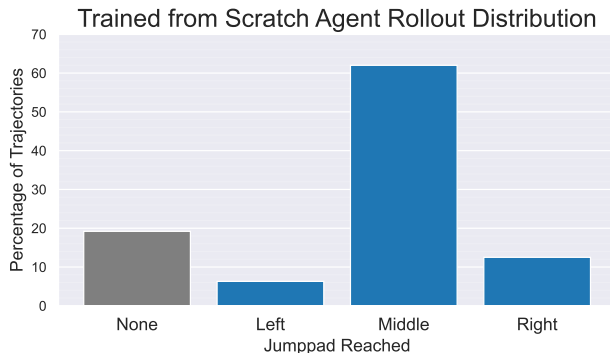


Figure 5. Distribution of jump pads reached by an equivalent agent trained from scratch on the task-specific dataset used for supervised fine-tuning.

Perhaps surprisingly, we find that the agent without pre-training has a less diverse jump pad distribution, and a higher failure rate (around 20%, almost twice that of the pre-trained agent). This finding seems to go against conventional wisdom that only clean, relevant demonstrations should be used from the available data. Instead, these results corroborate similar findings for LLMs, in which pre-training on diverse data has been shown to enable more effective fine-tuning, effectively increasing the size of the fine-tuning data compared to training from scratch (Hernandez et al., 2021).

To understand the reason behind this difference, we reviewed videos of the two agents navigating towards the jump pads. We noticed that failures would often arise when an agent accumulates action error over its trajectory, a common challenge with imitation learning (Ross & Bagnell, 2010), causing it to miss the intended jump pad as shown in Figure 6. Since the fine-tuning dataset consists of only a small number of trajectories that hit the jump pad directly, the agent trained from scratch (without pre-training) has never seen that observation before, so therefore chooses the modal action (which is to move forwards) as it is now out of distribution. This causes it to run into the wall continuously until it times out, leading to failure (Fig. 6, left). On the other hand, the pre-trained agent would often hit the wall, and then turn around and hit the jump pad from behind (Fig. 6, right). This is because the more diverse pre-training data provides a common-sense behavior prior, allowing the agent to return to the fine-tuning distribution. These behaviors are demonstrated in the videos on our project webpage, and provide anecdotal but intuitive evidence for the benefits of unsupervised pre-training in the context of agents.



Figure 6. Screenshots of the agent after having missed the intended jump pad. Left: Agent without pre-training continues into wall. Right: Agent with pre-training turns around to return to jump pad.

We also perform a preliminary investigation of model scaling in Appendix E, by training additional models with an equivalent transformer architecture from scratch on this smaller task-specific dataset. We find that smaller models have a higher failure rate, providing evidence that larger model sizes lead to improved performance in our imitation learning task, even when trained only on this relatively small fine-tuning dataset. These findings are in agreement with more comprehensive recent work by Pearce et al. (2024). Furthermore, we see early indications that larger models also align more efficiently with reinforcement learning.

In summary, we find that large-scale pre-training provides general benefits to agents, analogous to LLMs.

3.4. Preference Modeling

The next stage in the standard procedure for training LLMs is to obtain human preference data on model responses. Here we deploy the fine-tuned agent in the environment to collect trajectories for preference labelling. This is analogous to generating multiple LLM responses to a prompt, but in this context the prompt becomes the initial observation

and optional context of previous observations and actions (or instructional text embeddings) provided. Similarly to LLMs, there are tradeoffs to be made in the diversity, quality and quantity of preferences (discussed further in Appendix J), but here we avoid such issues by utilizing synthetic preferences to isolate the effect of quantity. Additionally, this labeling could potentially be automated using recent VLMs, again leveraging ideas and developments from the LLM-as-a-Judge literature (Zheng et al., 2023; Li et al., 2024).

Online Rollouts: We use the evaluation procedure described in Section 3.2 to generate a dataset of 2400 on-policy trajectories, divided into 1000 trajectories for training and 1400 for evaluation. Similarly to LLMs, the temperature of the softmax sampling of the policy for action selection can be increased to generate more diverse behaviors from the agent for easier comparison, but here we found the behavior to be diverse enough with a default temperature of one.

Generating Preferences: We use synthetic preferences to rank trajectories based on the primary jump pad (JP) criteria:

Given JP Reached \succ Other JP Reached \succ No JP Reached

Within each of these categories, we further rank by duration, preferring shorter trajectories. By selecting subsets of the training trajectories, we can investigate how reward model performance scales with number of comparisons (which is a proxy for human labeling time, often the main bottleneck for RLHF). A preference dataset P is then created by considering all pairwise comparisons of trajectories τ using the criteria above, i.e. $(\tau_A \succ \tau_B) \in P \forall \tau_A, \tau_B \in \tau$ if $\tau_A \succ \tau_B$.

3.5. Do modern reward-modeling practices apply in the context of agents?

A reward model is then trained on this dataset to predict rewards in accordance with preferences, as described below. Previous work on RLHF for agents has generally relied on independent (often linear) reward models (Knox & Stone, 2008; Christiano et al., 2017). However, recent work on LLMs has demonstrated that reward models using the pre-trained or fine-tuned policy model with the action classification head replaced with a scalar regression head generally perform better (Stiennon et al., 2020), and also improve with scale (Ouyang et al., 2022; Touvron et al., 2023). It is hypothesized that this is because the pre-training enables the reward model to better distinguish behaviors for reward assignment without the trajectory over-fitting that would occur with the equivalent model otherwise (Ziegler et al., 2020). We investigate this potential for representation transfer in the context of visual input agents in this section.

Procedure: We use the standard Bradley-Terry (Bradley & Terry, 1952) modeling procedure to train a reward model \hat{r} from these pairwise preferences, following Christiano et al. (2017). Specifically, we interpret trajectory rewards

as preference rankings analogous to Elo ratings (Elo, 1978) developed for chess, such that the annotator’s probability of preferring a trajectory depends exponentially on the trajectory reward difference. We can then fit the reward model by minimizing the cross-entropy between these probabilities and the preference labels, which gives the loss function:

$$\mathcal{L}(\hat{r}) = \sum_{(\tau_w, \tau_l) \in P} -\log \left(\sigma(\hat{r}(\tau_w) - \hat{r}(\tau_l)) \right) \quad (1)$$

where σ is the sigmoid function and (τ_w, τ_l) are the trajectories being compared, with τ_w being the winning (preferred) trajectory and τ_l being the losing trajectory. Since the reward model is only trained on comparisons, the scale of the predicted rewards is arbitrary. As a result, we found the need to apply a small amount of $L2$ regularization to prevent the scale of the rewards becoming overly large for the best and worst trajectories. We further empirically normalize the reward model after training using the max and min of predicted rewards over the training trajectories to scale our reward model output to be in the range $\hat{r} \in [0, 1]$.

Architecture: Following the LLM procedure to use the agent model for the reward model initialization, we take the output embeddings of the fine-tuned transformer at each timestep as input to an MLP. This outputs a scalar return for use in the loss function in Equation 1. As a baseline, we considered training a reward model with an equivalent architecture end-to-end, but found this led to trivial over-fitting and negligible validation performance. Instead, we use a frozen randomly initialized encoder to provide embeddings for each timestep, which are fed into an equivalent MLP.

Results: Each reward model is applied to our held-out test trajectories. We compute pairwise preferences, and compare to ground-truth preferences to obtain a test accuracy. Reward model performances are shown in Figure 7.

We find that reward model accuracy increases approximately logarithmically with comparisons, although the random projection reward models have high variance. Additionally, the reward models utilizing the agent model perform better than the reward models using random projections across the full range of comparison sizes, confirming the relevance of the imitation learning representations. Importantly, this transfer makes it possible to train a reward model from visual input to achieve over 90% preference accuracy with only ~ 100 comparisons. While this is a relatively simple task, we note that this would correspond to less than 1 hour of labeling time, demonstrating the feasibility of this approach for aligning pixel-based agents from trajectory videos.

In summary, we find evidence of representation transfer between imitation learning and preference modeling, that enables feedback-efficient reward modeling for aligning pixel-based agents.

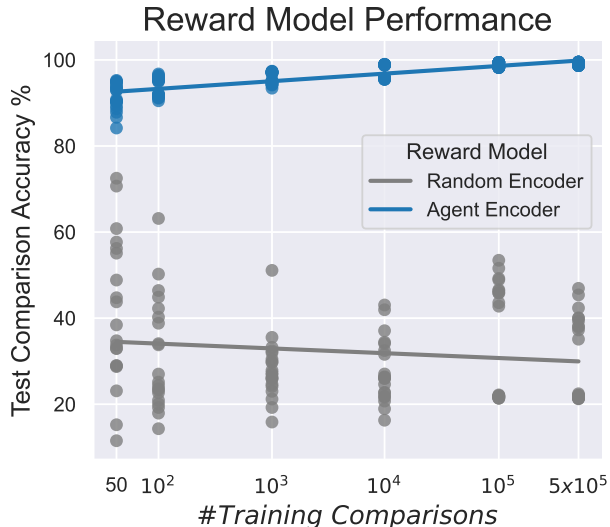


Figure 7. Reward model test accuracies against number of training comparisons for random and agent-initialized models.

3.6. Aligning the Agent with the Reward Model

Procedure: Finally, we align our agent with the preferences captured by our reward models. We run our fine-tuned agent in the environment as for evaluation to generate online trajectories. After each trajectory is complete, we apply our reward model to the trajectory to generate a reward. We use this reward as the return for the trajectory and update our agent policy π using REINFORCE (Williams, 1992). We discuss the motivation behind this choice in Appendix G.

For our experiments we ran our agent online for around a day of real-time gameplay, corresponding to 600 parameter updates (see Appendix C for details). The standard approach in LLM alignment would be to fine-tuning the entire network with an additional KL divergence term to regularize the optimized policy towards the initial fine-tuned policy (Touvron et al., 2023; Bai et al., 2022), but for our proof of concept we simply fine-tune the last layer for efficiency. We also note that approaches such as Low-Rank Adaption (LoRA) (Hu et al., 2021) used for fine-tuning LLMs could also be used here for memory-efficient alignment of a large base model with an individual’s preferences.

3.6.1. ALIGNING AGENT TOWARDS LEFT JUMPPAD

We begin by aligning our agent to reach the left jumppad. We plot the average success rate of reaching the left jumppad against the number of episodes in Figure 8, for reward models that have been trained on 100 up to 500k comparisons. We see that all of our reward models are sufficient to align our agent to consistently reach the left jumppad, with reward models trained on more data (with higher test performances) generally leading to better alignment.

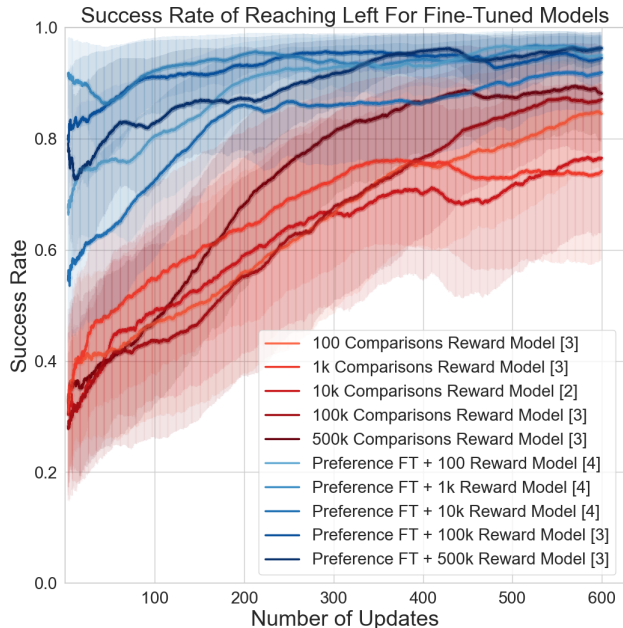


Figure 8. Left jumppad success rate during online alignment. Standard errors shaded, and number of seeds shown in legend. We see: 1) Higher accuracy reward models (darker) generally lead to better alignment, 2) Preference fine-tuning before online alignment (blue) improves performance for all reward models.

However, we see that the agents take most of the 600 updates to fully align, corresponding to a day of real-time training. To improve this efficiency, we again take inspiration from the LLM literature and consider the addition of a *preference fine-tuning* phase in which we first further fine-tune on the preferred trajectories. Specifically, we apply the reward model to the training trajectories and take the top 20% of trajectories by reward (corresponding to the preferred trajectories) and perform additional fine-tuning on these trajectories. This corresponds to a single iteration of Reinforced Self-Training (ReST) (Gulcehre et al., 2023), recently introduced to improve the efficiency of language model alignment. We find that this improves online performance for all reward models, shown in Figure 8.

3.6.2. ALIGNING AGENT TOWARDS RIGHT JUMPPAD

We now consider aligning our agent towards the right jumppad. Since this task is seemingly of identical difficulty, we would expect to be able to align the agent similarly. However, we found that our agents did not align as quickly towards the right jumppad, and in the absence of preference fine-tuning only reached around a $\sim 40\%$ success rate after one day of training, as shown in Figure 9.

We investigate this discrepancy in Appendix H, and find that it arises from an imbalance in spawn locations that makes it difficult for the agent to receive positive reward from certain

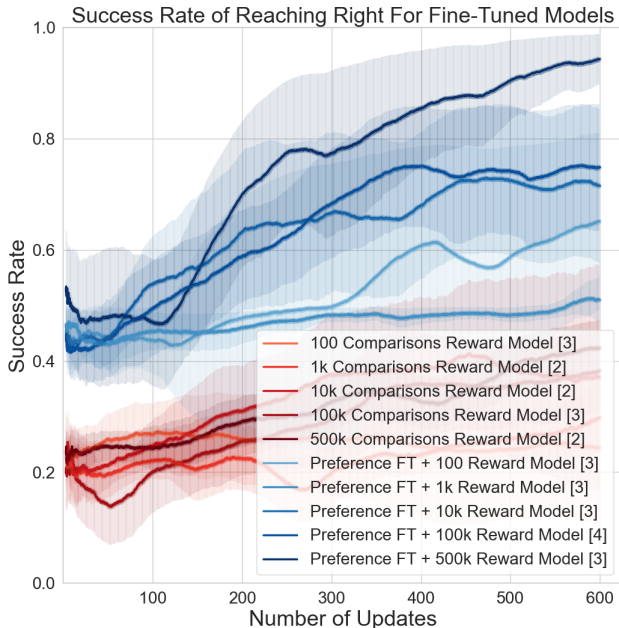


Figure 9. Right jumppad success rate during online alignment. Standard errors shaded, and number of seeds shown in legend. Similar trends hold to Figure 8, with the benefits of preference fine-tuning (blue) even more prominent, but overall alignment is less effective.

spawns. However, the addition of preference fine-tuning before online alignment helps to mitigate this imbalance, as shown in Figure 9, since it modifies the agent to produce more of the preferred behaviors that achieve reward before online alignment. This enabled us to completely align the agent right with the same training budget, as shown by the final jumppad distributions in Appendix I. This further demonstrates the benefits of our proposed additional stage of preference fine-tuning. However, this is just one possible strategy to improve alignment efficiency from the LLM literature. Many other approaches, such as Direct Preference Optimization (DPO) (Rafailov et al., 2023) could also be incorporated to alleviate the need for costly on-policy, online alignment. However, removing the need for online learning entirely is likely to be challenging, as discussed in Appendix D, and has been recently demonstrated in the context of LLMs (Xu et al., 2024).

In summary, we find that agents can be aligned to behave in accordance with human preferences by leveraging equivalent approaches to those used for modern LLMs, with similar benefits and effectiveness.

3.7. Summary of Agent Alignment

To visualize the gradual alignment of our agent, we provide a heatmap of agent trajectories at each stage of the alignment pipeline in Figure 10. This demonstrates how pre-training,

fine-tuning and RL(HF) can be used to reliably achieve behaviors that would not be possible with imitation learning (due to finite demonstrations) or reinforcement learning (due to lack of dense reward) alone. Videos of our agent at each stage are provided at: <https://adamjolley.github.io/aligning-agents-like-llms>.

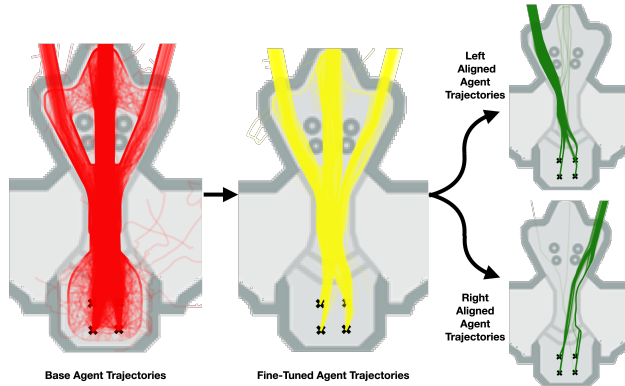


Figure 10. Heatmap of our agent’s trajectories at each stage of the alignment pipeline. Each stage shows 1000 trajectories.

4. Alternative Views and Broader Outlook

Our proof-of-concept provides evidence of the benefits of multi-stage training over imitation or reinforcement learning alone. However, an alternative view to our position might be that rather than training agents like LLMs, *LLMs should be used as agents directly*. There has indeed been significant progress in the development of LLM agents in recent years (Xi et al., 2023; Wang et al., 2024), including for low-level control (Yang et al., 2024; Brohan et al., 2023; Ahn et al., 2022; Driess et al., 2023; Tang et al., 2023).

However, multi-modal LLMs still struggle with low-level decision-making in complex environments such as video games, with recent work demonstrating that these models are a long way from human performance in these environments, even with significant amounts of gameplay data provided for in-context learning (Waytowich et al., 2024). In particular, Paglieri et al. (2024) recently demonstrated that LLM agents understandably struggle with experience-based aspects such as spatial reasoning, systematic exploration, long-term planning, understanding environment dynamics, and the ‘knowing-doing’ gap. In fact, LMAct (Ruoss et al., 2024) concludes “*Our work thus adds another piece to the growing literature that finds difficulties that LMs can have with translating declarative knowledge into effective acting (know-how) in some interactive decision-making tasks.*”

We argue that for tasks such as playing a 3D AAA video game, requiring fine-grained control of a gamepad controller at 10Hz, this problem will not simply go away with scale, and obtaining competent embodied agents will instead require training directly on interaction data. Just as human proficiency in video games and physical tasks depends more

on experience than intellectual capabilities, our position is that LLM agents will never be as capable as agents trained directly on interaction data, since they lack the common-sense behavioral priors necessary for low-level control.

In our proof-of-concept, we considered training an agent on general gameplay data before fine-tuning on a specific task. However, more generally, we could envision training a gaming foundation agent across a range of games (using our unified pixel observation space and gamepad controller action space), which could then be fine-tuned and aligned for a particular game. Similarly, while we primarily consider video games, we believe the modern LLM training paradigm (described more generally in Appendix A) could also be applied to training decision-making agents in other domains such as robotics. This could enable more general and robust agents, leveraging the impressive progress in LLMs while avoiding the fundamental limitations of LLM agents trained without real-world interaction data.

Finally, as LLMs inevitably continue to evolve, the developments can continue to be transferred to agents. For example, recent progress on improving LLM reasoning via process (Lightman et al., 2023) or outcome rewards (Lambert et al., 2024; DeepSeek-AI et al., 2025), or inference-time scaling (OpenAI et al., 2024), can be incorporated into this framework simply as conventional RL with environment rewards and search. But by making this stage the ‘cherry-on-the-cake’ (LeCun, 2016) rather than the sole training procedure, we can avoid many of the difficulties traditionally associated with RL, to obtain more general, robust and useful agents.

5. Conclusions

In this paper, we have taken the position that general agents should be trained like large language models. We have provided evidence for our position by following the LLM paradigm to train an agent from pixels to perform a desired behavior on a 3D AAA game as a proof-of-concept. This behavior would be difficult to achieve reliably with imitation learning or RL alone, demonstrating the value of each stage of the standard LLM training pipeline in the context of agents. We believe there is potential for many other recent developments in LLMs to transfer to decision-making agents, such as optimal dataset compositions, scaling laws, architectural and context improvements, post-training alignment procedures, and inference-time scaling. This will likely open up many exciting avenues of research in the coming years that have the potential to address many long-standing limitations and open-problems for decision-making agents. We hope our paper provides a framework for such research, and encourages communication and collaboration between the LLM and decision-making agent communities, to enable shared insights and provide a path towards more general and reliable agents for real-world applications.

Acknowledgements

This project was done during an internship with the Game Intelligence Team at Microsoft Research Cambridge. We are grateful to Ninja Theory and Microsoft for their support with the project. Thank you to Yuhan Cao and Dave Bignell for implementation and infrastructure support, Sam Devlin for advice and guidance, and particularly Tabish Rashid for supervising the internship and seeing the project through to completion. In addition to the authors, thank you to the whole team, including Anssi Kanervisto, Gunshi Gupta, Katja Hofmann, Lukas Schäfer, Raluca Georgescu, Sergio Valcarcel Macua, Shanzheng Tan, Tarun Gupta, Tim Pearce and Eloi Alonso for a great internship. Thank you also to Amos Storkey, Tom Lee, Trevor McInroe and Rich Turner for insightful discussions. Outside of the internship, Adam Jelley is supported by Microsoft Research and EP-SRC through Microsoft’s PhD Scholarship Programme.

Impact Statement

This paper presents work whose goal is to advance the field of machine learning, in particular decision-making agents. While these agents could have many positive impacts, ensuring the safety of such agents is crucial. Aligning agents with human preferences is a prominent approach to obtaining helpful and harmless agents, but this procedure has known open problems and limitations (Casper et al., 2023). Video games therefore provide an important test bed for such research, and we hope work such as ours can mitigate risks and provide insights in a safe environment that may generalize to other more real-world applications such as robotics.

References

- Abramson, J., Ahuja, A., Carnevale, F., Georgiev, P., Goldin, A., Hung, A., Landon, J., Lhotka, J., Lillicrap, T., Muldal, A., Powell, G., Santoro, A., Scully, G., Srivastava, S., von Glehn, T., Wayne, G., Wong, N., Yan, C., and Zhu, R. Improving Multimodal Interactive Agents with Reinforcement Learning from Human Feedback, November 2022. URL <http://arxiv.org/abs/2211.11602>. arXiv:2211.11602 [cs].
- Ahmadian, A., Cremer, C., Gallé, M., Fadaee, M., Kreutzer, J., Üstün, A., and Hooker, S. Back to Basics: Revisiting REINFORCE Style Optimization for Learning from Human Feedback in LLMs, February 2024. URL <http://arxiv.org/abs/2402.14740>. arXiv:2402.14740 [cs].
- Ahn, M., Brohan, A., Brown, N., Chebotar, Y., Cortes, O., David, B., Finn, C., Fu, C., Gopalakrishnan, K., Hausman, K., Herzog, A., Ho, D., Hsu, J., Ibarz, J., Ichter, B., Irpan, A., Jang, E., Ruano, R. J., Jeffrey, K., Jesmonth, S., Joshi, N. J., Julian, R., Kalashnikov, D., Kuang, Y., Lee, K.-H., Levine, S., Lu, Y., Luu, L., Parada, C., Pastor, P., Quiambao, J., Rao, K., Rettinghouse, J., Reyes, D., Sermanet, P., Sievers, N., Tan, C., Toshev, A., Vanhoucke, V., Xia, F., Xiao, T., Xu, P., Xu, S., Yan, M., and Zeng, A. Do As I Can, Not As I Say: Grounding Language in Robotic Affordances, August 2022. URL <http://arxiv.org/abs/2204.01691>. arXiv:2204.01691 [cs].
- Aytemiz, B., Jacob, M., and Devlin, S. Acting with Style: Towards Designer-centred Reinforcement Learning for the Video Games Industry. In *CHI 2021 Workshop on Reinforcement Learning for Humans, Computer, and Interaction (RLAHCI)*. Association for Computing Machinery (ACM), May 2021. URL <https://www.microsoft.com/en-us/research/publication/acting-with-style-towards-designer-centred-reinforcement-learning-for-the-video-games-industry/>.
- Ba, J. L., Kiros, J. R., and Hinton, G. E. Layer Normalization, July 2016. URL <http://arxiv.org/abs/1607.06450>. arXiv:1607.06450 [cs, stat].
- Bai, Y., Jones, A., Ndousse, K., Askell, A., Chen, A., Das-Sarma, N., Drain, D., Fort, S., Ganguli, D., Henighan, T., Joseph, N., Kadavath, S., Kernion, J., Conerly, T., El-Showk, S., Elhage, N., Hatfield-Dodds, Z., Hernandez, D., Hume, T., Johnston, S., Kravec, S., Lovitt, L., Nanda, N., Olsson, C., Amodei, D., Brown, T., Clark, J., McCandlish, S., Olah, C., Mann, B., and Kaplan, J. Training a Helpful and Harmless Assistant with Reinforcement Learning from Human Feedback, April 2022. URL <http://arxiv.org/abs/2204.05862>. arXiv:2204.05862 [cs].
- Baker, B., Akkaya, I., Zhokhov, P., Huizinga, J., Tang, J., Ecoffet, A., Houghton, B., Sampedro, R., and Clune, J. Video PreTraining (VPT): Learning to Act by Watching Unlabeled Online Videos, June 2022. URL <http://arxiv.org/abs/2206.11795>. arXiv:2206.11795 [cs].
- Banerjee, D., Singh, P., Avadhanam, A., and Srivastava, S. Benchmarking LLM powered Chatbots: Methods and Metrics, August 2023. URL <http://arxiv.org/abs/2308.04624>. arXiv:2308.04624 [cs].
- Beltagy, I., Peters, M. E., and Cohan, A. Longformer: The Long-Document Transformer, December 2020. URL <http://arxiv.org/abs/2004.05150>. arXiv:2004.05150 [cs].
- Bennett, J., Lanning, S., and Netflix, N. The Netflix Prize. January 2009.

- Bousmalis, K., Vezzani, G., Rao, D., Devin, C., Lee, A. X., Bauza, M., Davchev, T., Zhou, Y., Gupta, A., Raju, A., Laurens, A., Fantacci, C., Dalibard, V., Zambelli, M., Martins, M., Pevcevicute, R., Blokzijl, M., Denil, M., Batchelor, N., Lampe, T., Parisotto, E., Żoźna, K., Reed, S., Colmenarejo, S. G., Scholz, J., Abdolmaleki, A., Groth, O., Regli, J.-B., Sushkov, O., Rothörl, T., Chen, J. E., Aytar, Y., Barker, D., Ortiz, J., Riedmiller, M., Springenberg, J. T., Hadsell, R., Nori, F., and Heess, N. RoboCat: A Self-Improving Generalist Agent for Robotic Manipulation, December 2023. URL <http://arxiv.org/abs/2306.11706>. arXiv:2306.11706 [cs].
- Bradley, R. A. and Terry, M. E. Rank Analysis of Incomplete Block Designs: I. The Method of Paired Comparisons. *Biometrika*, 39(3/4):324–345, 1952. ISSN 0006-3444. doi: 10.2307/2334029. URL <https://www.jstor.org/stable/2334029>. Publisher: [Oxford University Press, Biometrika Trust].
- Brohan, A., Brown, N., Carbajal, J., Chebotar, Y., Dabis, J., Finn, C., Gopalakrishnan, K., Hausman, K., Herzog, A., Hsu, J., Ibarz, J., Ichter, B., Irpan, A., Jackson, T., Jesmonth, S., Joshi, N. J., Julian, R., Kalashnikov, D., Kuang, Y., Leal, I., Lee, K.-H., Levine, S., Lu, Y., Malla, U., Manjunath, D., Mordatch, I., Nachum, O., Parada, C., Peralta, J., Perez, E., Pertsch, K., Quiambao, J., Rao, K., Ryoo, M., Salazar, G., Sanketi, P., Sayed, K., Singh, J., Sontakke, S., Stone, A., Tan, C., Tran, H., Vanhoucke, V., Vega, S., Vuong, Q., Xia, F., Xiao, T., Xu, P., Xu, S., Yu, T., and Zitkovich, B. RT-1: Robotics Transformer for Real-World Control at Scale, December 2022. URL <http://arxiv.org/abs/2212.06817>. arXiv:2212.06817 [cs].
- Brohan, A., Brown, N., Carbajal, J., Chebotar, Y., Chen, X., Choromanski, K., Ding, T., Driess, D., Dubey, A., Finn, C., Florence, P., Fu, C., Arenas, M. G., Gopalakrishnan, K., Han, K., Hausman, K., Herzog, A., Hsu, J., Ichter, B., Irpan, A., Joshi, N., Julian, R., Kalashnikov, D., Kuang, Y., Leal, I., Lee, L., Lee, T.-W. E., Levine, S., Lu, Y., Michalewski, H., Mordatch, I., Pertsch, K., Rao, K., Reymann, K., Ryoo, M., Salazar, G., Sanketi, P., Sermanet, P., Singh, J., Singh, A., Soricut, R., Tran, H., Vanhoucke, V., Vuong, Q., Wahid, A., Welker, S., Wohlhart, P., Wu, J., Xia, F., Xiao, T., Xu, P., Xu, S., Yu, T., and Zitkovich, B. RT-2: Vision-Language-Action Models Transfer Web Knowledge to Robotic Control, July 2023. URL <http://arxiv.org/abs/2307.15818>. arXiv:2307.15818 [cs].
- Casper, S., Davies, X., Shi, C., Gilbert, T. K., Scheurer, J., Rando, J., Freedman, R., Korbak, T., Lindner, D., Freire, P., Wang, T., Marks, S., Segerie, C.-R., Carroll, M., Peng, A., Christoffersen, P., Damani, M., Slocum, S., Anwar, U., Siththaranjan, A., Nadeau, M., Michaud, E. J., Pfau, J., Krasheninnikov, D., Chen, X., Langosco, L., Hase, P., Bıyık, E., Dragan, A., Krueger, D., Sadigh, D., and Hadfield-Menell, D. Open Problems and Fundamental Limitations of Reinforcement Learning from Human Feedback, July 2023. URL <http://arxiv.org/abs/2307.15217>. arXiv:2307.15217 [cs].
- Chen, L., Lu, K., Rajeswaran, A., Lee, K., Grover, A., Laskin, M., Abbeel, P., Srinivas, A., and Mordatch, I. Decision Transformer: Reinforcement Learning via Sequence Modeling. *arXiv:2106.01345 [cs]*, June 2021a. URL <http://arxiv.org/abs/2106.01345>. arXiv: 2106.01345.
- Chen, M., Radford, A., Child, R., Wu, J., Jun, H., Luan, D., and Sutskever, I. Generative Pretraining From Pixels. In *Proceedings of the 37th International Conference on Machine Learning*, pp. 1691–1703. PMLR, November 2020. URL <https://proceedings.mlr.press/v119/chen20s.html>. ISSN: 2640-3498.
- Chen, M., Tworek, J., Jun, H., Yuan, Q., Pinto, H. P. d. O., Kaplan, J., Edwards, H., Burda, Y., Joseph, N., Brockman, G., Ray, A., Puri, R., Krueger, G., Petrov, M., Khlaaf, H., Sastry, G., Mishkin, P., Chan, B., Gray, S., Ryder, N., Pavlov, M., Power, A., Kaiser, L., Bavarian, M., Winter, C., Tillet, P., Such, F. P., Cummings, D., Plappert, M., Chantzis, F., Barnes, E., Herbert-Voss, A., Guss, W. H., Nichol, A., Paino, A., Tezak, N., Tang, J., Babuschkin, I., Balaji, S., Jain, S., Saunders, W., Hesse, C., Carr, A. N., Leike, J., Achiam, J., Misra, V., Morikawa, E., Radford, A., Knight, M., Brundage, M., Murati, M., Mayer, K., Welinder, P., McGrew, B., Amodei, D., McCandlish, S., Sutskever, I., and Zaremba, W. Evaluating Large Language Models Trained on Code, July 2021b. URL <http://arxiv.org/abs/2107.03374>. arXiv:2107.03374 [cs].
- Christiano, P., Leike, J., Brown, T. B., Martic, M., Legg, S., and Amodei, D. Deep reinforcement learning from human preferences, July 2017. URL <http://arxiv.org/abs/1706.03741>. arXiv:1706.03741 [cs, stat].
- Chung, H. W., Hou, L., Longpre, S., Zoph, B., Tay, Y., Fedus, W., Li, Y., Wang, X., Dehghani, M., Brahma, S., Webson, A., Gu, S. S., Dai, Z., Suzgun, M., Chen, X., Chowdhery, A., Castro-Ros, A., Pellat, M., Robinson, K., Valter, D., Narang, S., Mishra, G., Yu, A., Zhao, V., Huang, Y., Dai, A., Yu, H., Petrov, S., Chi, E. H., Dean, J., Devlin, J., Roberts, A., Zhou, D., Le, Q. V., and Wei, J. Scaling Instruction-Finetuned Language Models, December 2022. URL <http://arxiv.org/abs/2210.11416>. arXiv:2210.11416 [cs].
- DeepSeek-AI, Guo, D., Yang, D., Zhang, H., Song, J., Zhang, R., Xu, R., Zhu, Q., Ma, S., Wang, P., Bi, X.,

- Zhang, X., Yu, X., Wu, Y., Wu, Z. F., Gou, Z., Shao, Z., Li, Z., Gao, Z., Liu, A., Xue, B., Wang, B., Wu, B., Feng, B., Lu, C., Zhao, C., Deng, C., Zhang, C., Ruan, C., Dai, D., Chen, D., Ji, D., Li, E., Lin, F., Dai, F., Luo, F., Hao, G., Chen, G., Li, G., Zhang, H., Bao, H., Xu, H., Wang, H., Ding, H., Xin, H., Gao, H., Qu, H., Li, H., Guo, J., Li, J., Wang, J., Chen, J., Yuan, J., Qiu, J., Li, J., Cai, J. L., Ni, J., Liang, J., Chen, J., Dong, K., Hu, K., Gao, K., Guan, K., Huang, K., Yu, K., Wang, L., Zhang, L., Zhao, L., Wang, L., Zhang, L., Xu, L., Xia, L., Zhang, M., Zhang, M., Tang, M., Li, M., Wang, M., Li, M., Tian, N., Huang, P., Zhang, P., Wang, Q., Chen, Q., Du, Q., Ge, R., Zhang, R., Pan, R., Wang, R., Chen, R. J., Jin, R. L., Chen, R., Lu, S., Zhou, S., Chen, S., Ye, S., Wang, S., Yu, S., Zhou, S., Pan, S., Li, S. S., Zhou, S., Wu, S., Ye, S., Yun, T., Pei, T., Sun, T., Wang, T., Zeng, W., Zhao, W., Liu, W., Liang, W., Gao, W., Yu, W., Zhang, W., Xiao, W. L., An, W., Liu, X., Wang, X., Chen, X., Nie, X., Cheng, X., Liu, X., Xie, X., Liu, X., Yang, X., Li, X., Su, X., Lin, X., Li, X. Q., Jin, X., Shen, X., Chen, X., Sun, X., Wang, X., Song, X., Zhou, X., Wang, X., Shan, X., Li, Y. K., Wang, Y. Q., Wei, Y. X., Zhang, Y., Xu, Y., Li, Y., Zhao, Y., Sun, Y., Wang, Y., Yu, Y., Zhang, Y., Shi, Y., Xiong, Y., He, Y., Piao, Y., Wang, Y., Tan, Y., Ma, Y., Liu, Y., Guo, Y., Ou, Y., Wang, Y., Gong, Y., Zou, Y., He, Y., Xiong, Y., Luo, Y., You, Y., Liu, Y., Zhou, Y., Zhu, Y. X., Xu, Y., Huang, Y., Li, Y., Zheng, Y., Zhu, Y., Ma, Y., Tang, Y., Zha, Y., Yan, Y., Ren, Z. Z., Ren, Z., Sha, Z., Fu, Z., Xu, Z., Xie, Z., Zhang, Z., Hao, Z., Ma, Z., Yan, Z., Wu, Z., Gu, Z., Zhu, Z., Liu, Z., Li, Z., Xie, Z., Song, Z., Pan, Z., Huang, Z., Xu, Z., Zhang, Z., and Zhang, Z. DeepSeek-R1: Incentivizing Reasoning Capability in LLMs via Reinforcement Learning, January 2025. URL <http://arxiv.org/abs/2501.12948>. arXiv:2501.12948 [cs].
- Devlin, S., Georgescu, R., Momennejad, I., Rzepecki, J., Zuzniga, E., Costello, G., Leroy, G., Shaw, A., and Hofmann, K. Navigation Turing Test (NTT): Learning to Evaluate Human-Like Navigation, July 2021. URL <http://arxiv.org/abs/2105.09637>. arXiv:2105.09637.
- Driess, D., Xia, F., Sajjadi, M. S. M., Lynch, C., Chowdhery, A., Ichter, B., Wahid, A., Tompson, J., Vuong, Q., Yu, T., Huang, W., Chebotar, Y., Sermanet, P., Duckworth, D., Levine, S., Vanhoucke, V., Hausman, K., Toussaint, M., Greff, K., Zeng, A., Mordatch, I., and Florence, P. PaLM-E: An Embodied Multimodal Language Model, March 2023. URL <http://arxiv.org/abs/2303.03378>. arXiv:2303.03378 [cs].
- Elo, A. E. *The Rating of Chessplayers, Past and Present*. Arco Pub., 1978. ISBN 978-0-668-04721-0. Google-Books-ID: 8pMnAQAAMAAJ.
- Embodiment-Collaboration, O’Neill, A., Rehman, A., Gupta, A., Maddukuri, A., Gupta, A., Padalkar, A., Lee, A., Pooley, A., Gupta, A., Mandlkar, A., Jain, A., Tung, A., Bewley, A., Herzog, A., Irpan, A., Khazatsky, A., Rai, A., Gupta, A., Wang, A., Kolobov, A., Singh, A., Garg, A., Kembhavi, A., Xie, A., Brohan, A., Raffin, A., Sharma, A., Yavary, A., Jain, A., Balakrishna, A., Wahid, A., ..., Zhu, Y., Zhang, Y., Jiang, Y., Li, Y., Li, Y., Iwasawa, Y., Matsuo, Y., Ma, Z., Xu, Z., Cui, Z. J., Zhang, Z., Fu, Z., and Lin, Z. Open x-embodiment: Robotic learning datasets and RT-x models, 2024. URL <https://arxiv.org/abs/2310.08864>. arXiv:2310.08864 [cs.RO].
- Esser, P., Kulal, S., Blattmann, A., Entezari, R., Müller, J., Saini, H., Levi, Y., Lorenz, D., Sauer, A., Boesel, F., Podell, D., Dockhorn, T., English, Z., Lacey, K., Goodwin, A., Marek, Y., and Rombach, R. Scaling Rectified Flow Transformers for High-Resolution Image Synthesis, March 2024. URL <http://arxiv.org/abs/2403.03206>. arXiv:2403.03206 [cs].
- Gemini-Team, G., Anil, R., Borgeaud, S., Alayrac, J.-B., Yu, J., Soricut, R., Schalkwyk, J., Dai, A. M., Hauth, A., Millican, K., Silver, D., Johnson, M., Antonoglou, I., Schrittwieser, J., Glaese, A., Chen, J., Pitler, E., Lillicrap, T., Lazaridou, A., Firat, O., Molloy, J., Isard, M., Barham, P. R., Hennigan, T., Lee, B., ..., Dean, J., and Vinyals, O. Gemini: a family of highly capable multimodal models, 2024. URL <https://arxiv.org/abs/2312.11805>. arXiv:2312.11805 [cs.CL].
- Google Deepmind, G. T. Gemma: Open Models Based on Gemini Research and Technology. Technical report, February 2024. URL <https://storage.googleapis.com/deepmind-media/gemma/gemma-report.pdf>.
- Gulcehre, C., Paine, T. L., Srinivasan, S., Konyushkova, K., Weerts, L., Sharma, A., Siddhant, A., Ahern, A., Wang, M., Gu, C., Macherey, W., Doucet, A., Firat, O., and de Freitas, N. Reinforced Self-Training (ReST) for Language Modeling, August 2023. URL <http://arxiv.org/abs/2308.08998>. arXiv:2308.08998 [cs].
- Hendrycks, D. and Gimpel, K. Gaussian Error Linear Units (GELUs), June 2023. URL <http://arxiv.org/abs/1606.08415>. arXiv:1606.08415 [cs].
- Hernandez, D., Kaplan, J., Henighan, T., and McCandlish, S. Scaling Laws for Transfer, February 2021. URL <http://arxiv.org/abs/2102.01293>. arXiv:2102.01293 [cs].
- Hester, T., Vecerik, M., Pietquin, O., Lanctot, M., Schaul, T., Piot, B., Horgan, D., Quan, J., Sendonaris, A., Dulac-Arnold, G., Osband, I., Agapiou, J., Leibo, J. Z., and Gruslys, A. Deep Q-learning from Demonstrations,

- November 2017. URL <http://arxiv.org/abs/1704.03732>. arXiv:1704.03732 [cs].
- Hoffmann, J., Borgeaud, S., Mensch, A., Buchatskaya, E., Cai, T., Rutherford, E., Casas, D. d. L., Hendricks, L. A., Welbl, J., Clark, A., Hennigan, T., Noland, E., Millican, K., Driessche, G. v. d., Damoc, B., Guy, A., Osindero, S., Simonyan, K., Elsen, E., Rae, J. W., Vinyals, O., and Sifre, L. Training Compute-Optimal Large Language Models, March 2022. URL <http://arxiv.org/abs/2203.15556>. arXiv:2203.15556 [cs].
- Hu, E. J., Shen, Y., Wallis, P., Allen-Zhu, Z., Li, Y., Wang, S., Wang, L., and Chen, W. LoRA: Low-Rank Adaptation of Large Language Models, October 2021. URL <http://arxiv.org/abs/2106.09685>. arXiv:2106.09685 [cs].
- Hu, J., Tao, L., Yang, J., and Zhou, C. Aligning Language Models with Offline Reinforcement Learning from Human Feedback, August 2023. URL <http://arxiv.org/abs/2308.12050>. arXiv:2308.12050 [cs] version: 1.
- Ibarz, B., Leike, J., Pohlen, T., Irving, G., Legg, S., and Amodei, D. Reward learning from human preferences and demonstrations in Atari. In *Advances in Neural Information Processing Systems*, volume 31. Curran Associates, Inc., 2018. URL <https://proceedings.neurips.cc/paper/2018/hash/8cbe9ce23f42628c98f80fa0fac8b19a-Abstract.html>.
- Kaplan, J., McCandlish, S., Henighan, T., Brown, T. B., Chess, B., Child, R., Gray, S., Radford, A., Wu, J., and Amodei, D. Scaling Laws for Neural Language Models, January 2020. URL <http://arxiv.org/abs/2001.08361>. arXiv:2001.08361 [cs, stat].
- Knox, B. and Stone, P. TAMER: Training an Agent Manually via Evaluative Reinforcement. In *2008 7th IEEE International Conference on Development and Learning*, pp. 292–297, Monterey, CA, August 2008. IEEE. ISBN 978-1-4244-2661-4. doi: 10.1109/DEVLRN.2008.4640845. URL <http://ieeexplore.ieee.org/document/4640845/>.
- Lambert, N., Morrison, J., Pyatkin, V., Huang, S., Ivison, H., Brahman, F., Miranda, L. J. V., Liu, A., Dziri, N., Lyu, S., Gu, Y., Malik, S., Graf, V., Hwang, J. D., Yang, J., Bras, R. L., Tafford, O., Wilhelm, C., Soldaini, L., Smith, N. A., Wang, Y., Dasigi, P., and Hajishirzi, H. TŪLU 3: Pushing Frontiers in Open Language Model Post-Training, November 2024. URL <http://arxiv.org/abs/2411.15124>. arXiv:2411.15124 [cs] version: 1.
- LeCun, Y. NIPS Invited Talk Predictive Learning, 2016. URL <https://nips.cc/virtual/2016/invited-talk/6197>.
- Lee, K., Smith, L., and Abbeel, P. PEBBLE: Feedback-Efficient Interactive Reinforcement Learning via Re-labeling Experience and Unsupervised Pre-training, June 2021. URL <http://arxiv.org/abs/2106.05091>. arXiv:2106.05091 [cs].
- Lee, K.-H., Nachum, O., Yang, M., Lee, L., Freeman, D., Xu, W., Guadarrama, S., Fischer, I., Jang, E., Michalewski, H., and Mordatch, I. Multi-Game Decision Transformers, October 2022. URL <http://arxiv.org/abs/2205.15241>. arXiv:2205.15241.
- Levine, S., Kumar, A., Tucker, G., and Fu, J. Offline Reinforcement Learning: Tutorial, Review, and Perspectives on Open Problems, November 2020. URL <http://arxiv.org/abs/2005.01643>. arXiv:2005.01643 [cs, stat].
- Lewis, P., Perez, E., Piktus, A., Petroni, F., Karpukhin, V., Goyal, N., Küttler, H., Lewis, M., Yih, W.-t., Rocktäschel, T., Riedel, S., and Kiela, D. Retrieval-Augmented Generation for Knowledge-Intensive NLP Tasks, April 2021. URL <http://arxiv.org/abs/2005.11401>. arXiv:2005.11401 [cs].
- Li, H., Dong, Q., Chen, J., Su, H., Zhou, Y., Ai, Q., Ye, Z., and Liu, Y. LLMs-as-Judges: A Comprehensive Survey on LLM-based Evaluation Methods, December 2024. URL <http://arxiv.org/abs/2412.05579>. arXiv:2412.05579 [cs].
- Lightman, H., Kosaraju, V., Burda, Y., Edwards, H., Baker, B., Lee, T., Leike, J., Schulman, J., Sutskever, I., and Cobbe, K. Let’s Verify Step by Step, May 2023. URL <http://arxiv.org/abs/2305.20050>. arXiv:2305.20050 [cs].
- Liu, Z., Mao, H., Wu, C.-Y., Feichtenhofer, C., Darrell, T., and Xie, S. A ConvNet for the 2020s, March 2022. URL <http://arxiv.org/abs/2201.03545>. arXiv:2201.03545 [cs].
- Loshchilov, I. and Hutter, F. Decoupled Weight Decay Regularization, January 2019. URL <http://arxiv.org/abs/1711.05101>. arXiv:1711.05101 [cs, math].
- Milani, S., Kanervisto, A., Ramanauskas, K., Schulhoff, S., Houghton, B., Mohanty, S., Galbraith, B., Chen, K., Song, Y., Zhou, T., Yu, B., Liu, H., Guan, K., Hu, Y., Lv, T., Malato, F., Leopold, F., Raut, A., Hautamäki, V., Melnik, A., Ishida, S., Henriques, J. F., Klassert, R., Laurito, W., Novoseller, E., Goecks, V. G., Waytowich, N., Watkins, D., Miller, J., and Shah, R. Towards Solving Fuzzy Tasks with Human Feedback: A

- Retrospective of the MineRL BASALT 2022 Competition, March 2023. URL <http://arxiv.org/abs/2303.13512>. arXiv:2303.13512 [cs].
- OpenAI. Introducing ChatGPT, 2022. URL <https://openai.com/blog/chatgpt>.
- OpenAI. GPT-4 Technical Report, March 2023. URL <http://arxiv.org/abs/2303.08774>. arXiv:2303.08774 [cs].
- OpenAI, Jaech, A., Kalai, A., Lerer, A., Richardson, A., El-Kishky, A., Low, A., Helyar, A., Madry, A., Beutel, A., Carney, A., Iftimie, A., Karpenko, A., Passos, A. T., Neitz, A., Prokofiev, A., Wei, A., Tam, A., Bennett, A., Kumar, A., Saraiva, A., Vallone, A., Duberstein, A., Kondrich, A., Mishchenko, A., Applebaum, A., Jiang, A., Nair, A., Zoph, B., Ghorbani, B., Rossen, B., Sokolowsky, B., Barak, B., McGrew, B., Minaiev, B., Hao, B., Baker, B., Houghton, B., McKinzie, B., Eastman, B., Lugaresi, C., Bassin, C., Hudson, C., Li, C. M., Bourcy, C. d., Voss, C., Shen, C., Zhang, C., Koch, C., Orsinger, C., Hesse, C., Fischer, C., Chan, C., Roberts, D., Kappler, D., Levy, D., Selsam, D., Dohan, D., Farhi, D., Mely, D., Robinson, D., Tsipras, D., Li, D., Oprica, D., Freeman, E., Zhang, E., Wong, E., Proehl, E., Cheung, E., Mitchell, E., Wallace, E., Ritter, E., Mays, E., Wang, F., Such, F. P., Raso, F., Leoni, F., Tsimpourlas, F., Song, F., Lohmann, F. v., Sulit, F., Salmon, G., Parascandolo, G., Chabot, G., Zhao, G., Brockman, G., Leclerc, G., Salman, H., Bao, H., Sheng, H., Andrin, H., Bagherinezhad, H., Ren, H., Lightman, H., Chung, H. W., Kivlichan, I., O’Connell, I., Osband, I., Gilaberte, I. C., Akkaya, I., Kostrikov, I., Sutskever, I., Kofman, I., Pachocki, J., Lennon, J., Wei, J., Harb, J., Twore, J., Feng, J., Yu, J., Weng, J., Tang, J., Yu, J., Candela, J. Q., Palermo, J., Parish, J., Heidecke, J., Hallman, J., Rizzo, J., Gordon, J., Uesato, J., Ward, J., Huizinga, J., Wang, J., Chen, K., Xiao, K., Singhal, K., Nguyen, K., Cobbe, K., Shi, K., Wood, K., Rimbach, K., Gu-Lemberg, K., Liu, K., Lu, K., Stone, K., Yu, K., Ahmad, L., Yang, L., Liu, L., Maksin, L., Ho, L., Fedus, L., Weng, L., Li, L., McCallum, L., Held, L., Kuhn, L., Kondraciuk, L., Kaiser, L., Metz, L., Boyd, M., Trebacz, M., Joglekar, M., Chen, M., Tintor, M., Meyer, M., Jones, M., Kaufer, M., Schwarzer, M., Shah, M., Yatbaz, M., Guan, M. Y., Xu, M., Yan, M., Glaese, M., Chen, M., Lampe, M., Malek, M., Wang, M., Fradin, M., McClay, M., Pavlov, M., Wang, M., Wang, M., Murati, M., Bavarian, M., Rohaninejad, M., McAleese, N., Chowdhury, N., Chowdhury, N., Ryder, N., Tezak, N., Brown, N., Nachum, O., Boiko, O., Murk, O., Watkins, O., Chao, P., Ashbourne, P., Izmailov, P., Zhokhov, P., Dias, R., Arora, R., Lin, R., Lopes, R. G., Gaon, R., Miyara, R., Leike, R., Hwang, R., Garg, R., Brown, R., James, R., Shu, R., Cheu, R., Greene, R., Jain, S., Altman, S., Toizer, S., Toyer, S., Miserendino, S., Agarwal, S., Hernandez, S., Baker, S., McKinney, S., Yan, S., Zhao, S., Hu, S., Santurkar, S., Chaudhuri, S. R., Zhang, S., Fu, S., Papay, S., Lin, S., Balaji, S., Sanjeev, S., Sidor, S., Broda, T., Clark, A., Wang, T., Gordon, T., Sanders, T., Patwardhan, T., Sottiaux, T., Degry, T., Dimson, T., Zheng, T., Garipov, T., Stasi, T., Bansal, T., Creech, T., Peterson, T., Eloundou, T., Qi, V., Kosaraju, V., Monaco, V., Pong, V., Fomenko, V., Zheng, W., Zhou, W., McCabe, W., Zaremba, W., Dubois, Y., Lu, Y., Chen, Y., Cha, Y., Bai, Y., He, Y., Zhang, Y., Wang, Y., Shao, Z., and Li, Z. OpenAI o1 System Card, December 2024. URL <http://arxiv.org/abs/2412.16720>. arXiv:2412.16720 [cs].
- Ostrovski, G., Castro, P. S., and Dabney, W. The Difficulty of Passive Learning in Deep Reinforcement Learning, October 2021. URL <http://arxiv.org/abs/2110.14020>. arXiv:2110.14020 [cs].
- Ouyang, L., Wu, J., Jiang, X., Almeida, D., Wainwright, C. L., Mishkin, P., Zhang, C., Agarwal, S., Slama, K., Ray, A., Schulman, J., Hilton, J., Kelton, F., Miller, L., Simens, M., Askell, A., Welinder, P., Christiano, P., Leike, J., and Lowe, R. Training language models to follow instructions with human feedback, March 2022. URL <http://arxiv.org/abs/2203.02155>. arXiv:2203.02155 [cs].
- Paglieri, D., Cupiał, B., Coward, S., Piterbarg, U., Wolczyk, M., Khan, A., Pignatelli, E., Kucinski, L., Pinto, L., Fergus, R., Foerster, J. N., Parker-Holder, J., and Rocktäschel, T. BALROG: Benchmarking Agentic LLM and VLM Reasoning On Games, November 2024. URL <http://arxiv.org/abs/2411.13543>. arXiv:2411.13543 [cs].
- Pearce, T., Rashid, T., Bignell, D., Georgescu, R., Devlin, S., and Hofmann, K. Scaling Laws for Pre-training Agents and World Models, December 2024. URL <http://arxiv.org/abs/2411.04434>. arXiv:2411.04434 [cs].
- Pomerleau, D. A. Efficient Training of Artificial Neural Networks for Autonomous Navigation. *Neural Computation*, 3(1):88–97, March 1991. ISSN 0899-7667. doi: 10.1162/neco.1991.3.1.88. Conference Name: Neural Computation.
- Radford, A., Narasimhan, K., Salimans, T., and Sutskever, I. Improving Language Understanding by Generative Pre-Training. 2018.
- Radford, A., Wu, J., Child, R., Luan, D., Amodei, D., and Sutskever, I. Language Models are Unsupervised Multi-task Learners. February 2019.

- Rafailov, R., Sharma, A., Mitchell, E., Ermon, S., Manning, C. D., and Finn, C. Direct Preference Optimization: Your Language Model is Secretly a Reward Model, May 2023. URL <http://arxiv.org/abs/2305.18290>. arXiv:2305.18290 [cs].
- Reed, S., Zolna, K., Parisotto, E., Colmenarejo, S. G., Novikov, A., Barth-Maron, G., Gimenez, M., Sulsky, Y., Kay, J., Springenberg, J. T., Eccles, T., Bruce, J., Razavi, A., Edwards, A., Heess, N., Chen, Y., Hadsell, R., Vinyals, O., Bordbar, M., and de Freitas, N. A Generalist Agent. Technical Report arXiv:2205.06175, arXiv, May 2022. URL <http://arxiv.org/abs/2205.06175>. arXiv:2205.06175 [cs] type: article.
- Ross, S. and Bagnell, D. Efficient Reductions for Imitation Learning. In *Proceedings of the Thirteenth International Conference on Artificial Intelligence and Statistics*, pp. 661–668. JMLR Workshop and Conference Proceedings, March 2010. URL <https://proceedings.mlr.press/v9/ross10a.html>. ISSN: 1938-7228.
- Ross, S., Gordon, G. J., and Bagnell, J. A. A Reduction of Imitation Learning and Structured Prediction to No-Regret Online Learning, March 2011. URL <http://arxiv.org/abs/1011.0686>. arXiv:1011.0686 [cs, stat].
- Ruoss, A., Pardo, F., Chan, H., Li, B., Mnih, V., and Genewein, T. LMAct: A Benchmark for In-Context Imitation Learning with Long Multimodal Demonstrations, December 2024. URL <http://arxiv.org/abs/2412.01441>. arXiv:2412.01441 [cs].
- Schulman, J., Wolski, F., Dhariwal, P., Radford, A., and Klimov, O. Proximal Policy Optimization Algorithms. *arXiv:1707.06347 [cs]*, August 2017. URL <http://arxiv.org/abs/1707.06347>. arXiv:1707.06347.
- Silver, D., Huang, A., Maddison, C. J., Guez, A., Sifre, L., van den Driessche, G., Schrittwieser, J., Antonoglou, I., Panneershelvam, V., Lanctot, M., Dieleman, S., Grewe, D., Nham, J., Kalchbrenner, N., Sutskever, I., Lillicrap, T., Leach, M., Kavukcuoglu, K., Graepel, T., and Hassabis, D. Mastering the game of Go with deep neural networks and tree search. *Nature*, 529(7587):484–489, January 2016. ISSN 1476-4687. doi: 10.1038/nature16961. URL <https://www.nature.com/articles/nature16961>. Bandiera_abtest: a Cg.type: Nature Research Journals Number: 7587 Primary_atype: Research Publisher: Nature Publishing Group Subject_term: Computational science;Computer science;Reward Subject_term.id: computational-science;computer-science;reward.
- SIMA-Team, Raad, M. A., Ahuja, A., Barros, C., Besse, F., Bolt, A., Bolton, A., Brownfield, B., Buttimore, G., Cant, M., Chakera, S., Chan, S. C. Y., Clune, J., Collister, A., Copeman, V., Cullum, A., Dasgupta, I., de Cesare, D., Di Trapani, J., Donchev, Y., Dunleavy, E., Engelage, M., Faulkner, R., Garcia, F., Gbadamosi, C., Gong, Z., Gonzales, L., Gupta, K., Gregor, K., Hallingstad, A. O., Harley, T., Haves, S., Hill, F., Hirst, E., Hudson, D. A., Hudson, J., Hughes-Fitt, S., Rezende, D. J., Jasarevic, M., Kamps, L., Ke, R., Keck, T., Kim, J., Knagg, O., Kopparapu, K., Lampinen, A., Legg, S., Lerchner, A., Limont, M., Liu, Y., Loks-Thompson, M., Marino, J., Cussons, K. M., Matthey, L., Mcloughlin, S., Mendolicchio, P., Merzic, H., Mitenkova, A., Moufarek, A., Oliveira, V., Oliveira, Y., Openshaw, H., Pan, R., Pappu, A., Platonov, A., Purkiss, O., Reichert, D., Reid, J., Richemond, P. H., Roberts, T., Ruscoe, G., Elias, J. S., Sandars, T., Sawyer, D. P., Scholtes, T., Simmons, G., Slater, D., Soyer, H., Strathmann, H., Stys, P., Tam, A. C., Teplyashin, D., Terzi, T., Vercelli, D., Vujatovic, B., Wainwright, M., Wang, J. X., Wang, Z., Wierstra, D., Williams, D., Wong, N., York, S., and Young, N. Scaling Instructable Agents Across Many Simulated Worlds, April 2024. URL <http://arxiv.org/abs/2404.10179>. arXiv:2404.10179 [cs].
- Spatharioti, S. E., Rothschild, D. M., Goldstein, D. G., and Hofman, J. M. Comparing Traditional and LLM-based Search for Consumer Choice: A Randomized Experiment, July 2023. URL <http://arxiv.org/abs/2307.03744>. arXiv:2307.03744 [cs].
- Stiennon, N., Ouyang, L., Wu, J., Ziegler, D., Lowe, R., Voss, C., Radford, A., Amodei, D., and Christiano, P. F. Learning to summarize with human feedback. In *Advances in Neural Information Processing Systems*, volume 33, pp. 3008–3021. Curran Associates, Inc., 2020. URL https://proceedings.neurips.cc/paper_files/paper/2020/hash/1f89885d556929e98d3ef9b86448f951-Abstract.html.
- Tang, Y., Yu, W., Tan, J., Zen, H., Faust, A., and Harada, T. SayTap: Language to Quadrupedal Locomotion, September 2023. URL <http://arxiv.org/abs/2306.07580>. arXiv:2306.07580 [cs].
- Touvron, H., Martin, L., Stone, K., Albert, P., Almahairi, A., Babaei, Y., Bashlykov, N., Batra, S., Bhargava, P., Bhosale, S., Bikel, D., Blecher, L., Ferrer, C. C., Chen, M., Cucurull, G., Esiobu, D., Fernandes, J., Fu, J., Fu, W., Fuller, B., Gao, C., Goswami, V., Goyal, N., Hartshorn, A., Hosseini, S., Hou, R., Inan, H., Kardas, M., Kerkez, V., Khabsa, M., Kloumann, I., Korenev, A., Koura, P. S., Lachaux, M.-A., Lavril, T., Lee, J., Liskovich, D., Lu, Y., Mao, Y., Martinet, X., Mihaylov, T., Mishra, P., Molybog,

- I., Nie, Y., Poulton, A., Reizenstein, J., Rungta, R., Saladi, K., Schelten, A., Silva, R., Smith, E. M., Subramanian, R., Tan, X. E., Tang, B., Taylor, R., Williams, A., Kuan, J. X., Xu, P., Yan, Z., Zarov, I., Zhang, Y., Fan, A., Kambadur, M., Narang, S., Rodriguez, A., Stojnic, R., Edunov, S., and Scialom, T. Llama 2: Open Foundation and Fine-Tuned Chat Models, July 2023. URL <http://arxiv.org/abs/2307.09288>. arXiv:2307.09288 [cs].
- Vecerik, M., Hester, T., Scholz, J., Wang, F., Pietquin, O., Piot, B., Heess, N., Rothörl, T., Lampe, T., and Riedmiller, M. Leveraging Demonstrations for Deep Reinforcement Learning on Robotics Problems with Sparse Rewards, October 2018. URL <http://arxiv.org/abs/1707.08817>. arXiv:1707.08817 [cs].
- Vinyals, O., Babuschkin, I., Czarnecki, W. M., Mathieu, M., Dudzik, A., Chung, J., Choi, D. H., Powell, R., Ewalds, T., Georgiev, P., Oh, J., Horgan, D., Kroiss, M., Danihelka, I., Huang, A., Sifre, L., Cai, T., Agapiou, J. P., Jaderberg, M., Vezhnevets, A. S., Leblond, R., Pohlen, T., Dalibard, V., Budden, D., Sulsky, Y., Molloy, J., Paine, T. L., Gulcehre, C., Wang, Z., Pfaff, T., Wu, Y., Ring, R., Yogatama, D., Wünsch, D., McKinney, K., Smith, O., Schaul, T., Lillicrap, T., Kavukcuoglu, K., Hassabis, D., Apps, C., and Silver, D. Grandmaster level in StarCraft II using multi-agent reinforcement learning. *Nature*, 575(7782):350–354, November 2019. ISSN 0028-0836, 1476-4687. doi: 10.1038/s41586-019-1724-z. URL <http://www.nature.com/articles/s41586-019-1724-z>.
- Wang, L., Ma, C., Feng, X., Zhang, Z., Yang, H., Zhang, J., Chen, Z., Tang, J., Chen, X., Lin, Y., Zhao, W. X., Wei, Z., and Wen, J.-R. A Survey on Large Language Model based Autonomous Agents. *Frontiers of Computer Science*, 18(6):186345, December 2024. ISSN 2095-2228, 2095-2236. doi: 10.1007/s11704-024-40231-1. URL <http://arxiv.org/abs/2308.11432>. arXiv:2308.11432 [cs].
- Waytowich, N. R., White, D., Sunbeam, M. D., and Goecks, V. G. Atari-GPT: Investigating the Capabilities of Multimodal Large Language Models as Low-Level Policies for Atari Games, August 2024. URL <http://arxiv.org/abs/2408.15950>. arXiv:2408.15950 [cs] version: 1.
- Williams, R. J. Simple statistical gradient-following algorithms for connectionist reinforcement learning. *Machine Learning*, 8(3):229–256, May 1992. ISSN 1573-0565. doi: 10.1007/BF00992696. URL <https://doi.org/10.1007/BF00992696>.
- Wirth, C., Akrou, R., Neumann, G., and Fürnkranz, J. A Survey of Preference-Based Reinforcement Learning Methods. 2017.
- Xi, Z., Chen, W., Guo, X., He, W., Ding, Y., Hong, B., Zhang, M., Wang, J., Jin, S., Zhou, E., Zheng, R., Fan, X., Wang, X., Xiong, L., Zhou, Y., Wang, W., Jiang, C., Zou, Y., Liu, X., Yin, Z., Dou, S., Weng, R., Cheng, W., Zhang, Q., Qin, W., Zheng, Y., Qiu, X., Huang, X., and Gui, T. The Rise and Potential of Large Language Model Based Agents: A Survey, September 2023. URL <http://arxiv.org/abs/2309.07864>. arXiv:2309.07864 [cs].
- Xu, J., Liu, X., Wu, Y., Tong, Y., Li, Q., Ding, M., Tang, J., and Dong, Y. ImageReward: Learning and Evaluating Human Preferences for Text-to-Image Generation, June 2023. URL <http://arxiv.org/abs/2304.05977>. arXiv:2304.05977 [cs].
- Xu, S., Fu, W., Gao, J., Ye, W., Liu, W., Mei, Z., Wang, G., Yu, C., and Wu, Y. Is DPO Superior to PPO for LLM Alignment? A Comprehensive Study, April 2024. URL <http://arxiv.org/abs/2404.10719>. arXiv:2404.10719 [cs] version: 1.
- Yang, Z., Liu, A., Liu, Z., Liu, K., Xiong, F., Wang, Y., Yang, Z., Hu, Q., Chen, X., Zhang, Z., Luo, F., Guo, Z., Li, P., and Liu, Y. Towards Unified Alignment Between Agents, Humans, and Environment, February 2024. URL <http://arxiv.org/abs/2402.07744>. arXiv:2402.07744 [cs].
- Zhang, R., Torabi, F., Warnell, G., and Stone, P. Recent Advances in Leveraging Human Guidance for Sequential Decision-Making Tasks. *Autonomous Agents and Multi-Agent Systems*, 35(2):31, October 2021. ISSN 1387-2532, 1573-7454. doi: 10.1007/s10458-021-09514-w. URL <http://arxiv.org/abs/2107.05825>. arXiv:2107.05825 [cs].
- Zheng, L., Chiang, W.-L., Sheng, Y., Zhuang, S., Wu, Z., Zhuang, Y., Lin, Z., Li, Z., Li, D., Xing, E. P., Zhang, H., Gonzalez, J. E., and Stoica, I. Judging LLM-as-a-Judge with MT-Bench and Chatbot Arena, December 2023. URL <http://arxiv.org/abs/2306.05685>. arXiv:2306.05685 [cs].
- Ziegler, D. M., Stiennon, N., Wu, J., Brown, T. B., Radford, A., Amodei, D., Christiano, P., and Irving, G. Fine-Tuning Language Models from Human Preferences, January 2020. URL <http://arxiv.org/abs/1909.08593>. arXiv:1909.08593 [cs, stat].

A. Discussion of General Procedure for Aligning Agents

We break down our procedure for training general decision-making agents (see Figure 1) into five steps:

1. Train a Base Imitation Learning Policy

The first ingredient for training large language models is to train a large, scalable transformer architecture with self-supervised next-token prediction on a diverse dataset of human text, to obtain a language prior. In the context of agents on modern console games, we interpret this as imitation learning to predict the next action taken in human gameplay data, to obtain a behavioral prior. Specifically this involves training the transformer autoregressively to learn a policy $p(a_t|o_t, a_{t-1}, \dots, o_{t-H}; e_t)$ with optional text conditioning e_t containing embedded context on the game, task or current goal. For the purpose of this work, we consider an agent trained on diverse data within a particular game, but note that given our unified observation and action spaces (visual observations and gamepad actions), it would also be possible to train across games, as explored in previous work (Reed et al., 2022; Lee et al., 2022).

2. Supervised Fine-Tune on a Task Relevant Dataset

The next step in the current LLM pipeline is to fine-tune the pre-trained ‘foundation’ model on task relevant data, such as instruction data (Chung et al., 2022). Pre-trained transformer models have been shown to fine-tune more effectively, essentially increasing the size of the fine-tuning data compared to training from scratch (Hernandez et al., 2021). For decision-making agents this involves fine-tuning by imitation learning on the task (or game) of interest. For specific behaviors, this could also consist of fine-tuning on demonstrations of the desired behavior by the game designer. The training procedure is equivalent to Step 1.

3. Generate Preference Data on Online Trajectories

Fine-tuned LLMs are subsequently prompted to generate multiple responses which are compared by human labelers to provide preferences. In the context of agents, the prompt becomes the initial observation (and optional context of previous observations, actions and/or textual instructions). The agent is then rolled out from a given initial start state multiple times to collect multiple trajectories. Similarly to LLMs, the temperature of the softmax sampling of the policy for action selection can be increased to generate more diverse behaviors from the agent for easier comparison. A human (e.g. game designer) then provides preferences on these trajectories, such as preferring trajectories where the agent plays in a certain style.

4. Train a Reward Model on Preferences

A reward model is then trained on these online trajectories, commonly using a Bradley Terry model (Bradley & Terry, 1952) for pairwise comparisons, so that the reward model provides higher reward for preferred trajectories. While this reward model is usually trained from scratch in the context of agents, the modern LLM procedure utilizes the pre-trained or fine-tuned policy model by replacing the action classification head with a scalar regression head. This enables the reward model to also benefit from the pre-training, and share the same knowledge as the agent to reduce out-of-distribution behaviors (Ziegler et al., 2020). This reward model should ideally capture general behavior preferences to provide more scalable feedback to the agent.

5. Align the Fine-tuned Model with the Reward Model

Finally the agent can be trained with online reinforcement learning to maximize the reward provided by the reward model, thereby aligning the agent with the game designer’s preferences. Since online reinforcement learning can be inefficient, various alternatives can be used, such as Direct Preference Optimization (DPO) (Rafailov et al., 2023) with an offline preference dataset or ReST (Gulcehre et al., 2023), but online learning is generally preferred (Xu et al., 2024). A common failure mode at this stage is reward model over-optimization, where the agent performs behaviors that maximize the reward model output but are not aligned with preferences (also known as reward hacking). If this occurs, regularization towards the original policy can be added or steps 3-5 can be repeated to generate new preferences on the reward hacking behavior which can be used to update the reward model. This may take multiple iterations (e.g. 5 reward model iterations were used for Llama 2 (Touvron et al., 2023)), to eventually obtain an aligned agent.

This procedure combines the benefits of large scale pre-training to obtain a widely generalizable agent, with the benefits of reinforcement learning from preferences to obtain an aligned agent. Furthermore, it also combines the benefits of offline learning to avoid the renown sample inefficiency of online reinforcement learning, with the benefits of online learning to alleviate the well-known problems associated with offline agents going out-of-distribution (Ross & Bagnell, 2010; Ross et al., 2011) by enabling some active online learning (Ostrovski et al., 2021) with a sensible behavioral prior.

Our procedure for aligning agents with preferences can also be summarized in algorithmic form:

Algorithm 1 Aligning Agents with Preferred Behaviours

Require: Large diverse dataset D , task specific dataset T , environment E , transformer policy π

- 1: Train policy π on large diverse dataset D with imitation learning (Pomerleau, 1991)

$$\mathcal{L}_U(\pi) = \mathbb{E}_D [-\log \pi(a_t^\tau | o_t^\tau, o_{t-1}^\tau, \dots)]$$

- 2: Fine-tune policy π on task specific dataset or demonstrations T

$$\mathcal{L}_{FT}(\pi) = \mathbb{E}_T [-\log \pi(a_t^\tau | o_t^\tau, o_{t-1}^\tau, \dots)]$$

- 3: Run fine-tuned policy π in environment and provide preferences on pairwise comparisons on online trajectories to obtain preference data $(\tau_A \succ \tau_B) \in P$
- 4: Initialise additional reward model \hat{r} from π and train on preferences P using Bradley-Terry model (Bradley & Terry, 1952)

$$\mathcal{L}(\hat{r}) = \sum_{(\tau_w, \tau_l) \in P} -\log \left(\sigma(\hat{r}(\tau_w) - \hat{r}(\tau_l)) \right)$$

- 5: Train fine-tuned policy π_{RL} using online reinforcement learning, using reward model \hat{r} to provide return for online trajectory τ to align agent with preferences. For example, using REINFORCE (Williams, 1992) with Kullback–Leibler divergence regularization parameterized by β :

$$\mathcal{L}_{RL}(\pi_{RL}) = -\mathbb{E}_{\pi_{RL}} \left[\sum_{t=1}^T \gamma^t \hat{r}(\tau) \log \pi_{RL}(a_t | o_t, \dots) - \beta \log \left(\frac{\pi_{RL}(a_t | o_t, \dots)}{\pi_{FT}(a_t | o_t, \dots)} \right) \right]$$

B. Bleeding Edge Game Human Data Collection

Human gameplay data was recorded as part of the regular gameplay process, in order to enable in-game functionality as well as to support research. In game, recordings allow players to view their past games to improve their skills and for entertainment. Games were recorded on the servers that hosted the games in the form of replay files, which include a representation of the internal game state and controller actions of all players.

Data collection was covered by an End User License Agreement (EULA) to which players agreed when logging in to play the game for the first time. Our use of the recorded human gameplay data for this specific research was governed by a data sharing agreement with the game studio, and approved by our institution’s IRB. To minimize risks regarding data privacy, any personally identifiable information (Xbox user ID) was removed when extracting the data used for this study from the original replays.

C. Architectures and Training Details

C.1. Base Model

For our base model ($\sim 103M$ parameters) we use a GPT-2 causal transformer architecture with 8 layers with 1024 hidden dim. Each attention layer has 8 heads, and the feedforward layers have a hidden dim of 4096.

Each image is resized to be of shape $128 \times 128 \times 3$, divided by 255 to put its values in $[0, 1]$, and is then fed into a convolutional encoder to map it to a 1024 dimensional vector.

The first layer of the conv net has kernels of shape 8×8 , with a stride of 4, and a padding of 3 and maps to 16 channel dimension. This is followed by 4 lots of ConvNext (Liu et al., 2022) and downsampling blocks (kernel of shape 3×3 , stride of 2, padding of 1, doubling the channel dimension). Finally, a LayerNorm (Ba et al., 2016) is applied to the output.

The transformer operates on sequences of 32 timesteps using learnt positional encodings. The output of the transformer is

layernormed, and then fed into an MLP with a single hidden layer of 1024 dimensions with a GELU (Hendrycks & Gimpel, 2023) non-linearity.

For our optimiser we use AdamW (Loshchilov & Hutter, 2019) with a learning rate of $1e - 4$ and a weight decay of $1e - 4$. We use a batch size of 256 with a learning rate warmup period of 1000 updates and a gradient clipping value of 1. We train with the same image augmentations as used by (Baker et al., 2022), and filter out all no-op actions.

We used 8 32GB Nvidia V100 GPUs for approximately 4 days to train the base model.

C.2. Fine-Tuning of Base Model

We train for 1500 batches of size 128 with a learning rate of $1e - 6$ with the same image augmentations and no-op filtering as for pre-training with 200 warmup steps.

We used 4 48GB Nvidia A6000 GPUs for less than 1 hour for fine-tuning.

C.3. Reward Models

Each trajectory is padded up to the maximum length of 100 (with black images) before being fed into the reward models.

For the `Random Encoder` model we randomly initialise a linear layer to randomly project the flattened values of the image to a 512 dimensional vector. This linear layer is not trained.

For the `Agent Encoder` model, we feed the trajectory into the fine-tuned agent and take the layernormed output of the transformer, corresponding to timesteps 0 up to 100, as 1024 dimensional embeddings. This is larger since it must capture the 32 context steps rather than just a single observation. The parameters of the fine-tuned agent are not trained.

For both models we then feed these vectors into an MLP with a GELU non-linearity and a hidden layer of 256 and an output dimension of 3. Each of the 100 3-dimensional vectors are concatenated together and then fed into another MLP with a GELU, 256 hidden dimension, and an output of 1.

To train the reward models we use a minibatch of size 2048, learning rate of $1e - 4$, and an L_2 regularisation penalty of 0.1. We train all models for 200 epochs, except for the largest training set size of 1000 trajectories which we train for 50 epochs.

After training, we compute the minimum and maximum outputs of the reward model on the training set. These are then used to normalise the output of the reward model to lie within $[0, 1]$.

We used 4 48GB Nvidia A6000 GPUs for a few hours in total for training all reward models.

C.4. Alignment Training

Preference Fine-Tuning: after training the reward model on its dataset of M trajectories (which result in a dataset of up to $N = (M)(M - 1)/2$ comparisons), we compute the reward for each of these M trajectories. We then sort them by magnitude, and take the top 20% of these as a smaller dataset to perform behaviour cloning on.

For this final step of BC, we use a learning rate of $1e - 5$ with 1000 updates on minibatches of size 256. We only train the parameters of the MLP after the transformer layers.

We again used 4 48GB Nvidia A6000 GPUs for less than an hour for preference fine-tuning.

Reinforcement Learning: in our experiments we use an undiscounted REINFORCE loss for 9600 episodes, using a batch size of 16 to give 600 parameter updates. Each episode is up to 100 timesteps or around 10s, so this corresponds to around 1 day of real time gameplay in total. We use a learning rate of $1e - 4$ and once again only train the parameters of the MLP after the transformer layers. If an error occurs during an episode’s rollout, we simply drop the samples from that episode and subsequently use a smaller batch size for the update.

We used 16 Standard NV12 machines (each with 2 Nvidia Tesla M60 GPUs for game rendering) on Azure Batch, requiring one machine around one day per seed for agent alignment.

The total compute used for the entire research project therefore represents of the order of weeks of total compute time, with preliminary experiments not included of the order of days of compute.

D. Discussion of Offline to Online Distribution Shift

The nature of using a real AAA video game is such that there is significant offline to online distribution shift between our offline training data and our online evaluation, as discussed in Section 3.3. Typical visual distribution shifts in our setting, due to character selection and customizable visual modifications, are shown below in Figure 11.



Figure 11. Screenshots of various characters with visual modifications contained within the general pre-training data. All are completely representative of the input provided to our agent (only 256×256 rather than 128×128 resolution). Figure (e) demonstrates the agent we use for online evaluation.

It is also well established that offline-only imitation learning usually suffers from online distribution drift, particularly when learning from pixels in a continuous and partially observable environment (Ross & Bagnell, 2010; Ross et al., 2011). Both of these sources of distribution drift often lead to significant accumulating error in an online trajectory. As a result, imitation learning agents may not consistently perform imitated behaviors online even if the loss has converged on the offline data. This challenge is fundamental to offline learning, as the agent cannot learn from its own observations and actions (Ostrovski et al., 2021). This motivates the need to have some online fine-tuning (in our case from preferences) to refine the policy to consistently perform the desired behavior online.

Figure 4 demonstrates that even after supervised fine-tuning on a dataset of trajectories that always reach a jumppad and involve the same character, a significant proportion of trajectories ($\sim 10\%$) do not reach any jumppad. However, after online fine-tuning, we are able to increase the overall success rate to nearly 100% as shown in Appendix I. We note that this is analogous to recent findings for LLMs that online training (when appropriately configured) can lead to performance improvements over offline-only training (Xu et al., 2024).

E. Preliminary Model Scaling and Alignment Analysis

E.1. Preliminary Model Scaling Analysis

To further justify the model size and investigate scaling properties of our transformer policy, we also trained smaller models of 4M and 25M parameters on our task-specific dataset, using the same procedure as above. The architecture of our 2 smaller models is identical to that of the base model described in Section C, except for:

- **~4M**: 4 layers with 256 hidden dims and 4 heads for each attention layer.
- **~25M**: 8 layers with 512 hidden dims and 8 heads for each attention layer.
- (**~103M**: 8 layers with 1024 hidden dims and 8 heads for each attention layer.)

Task-Specific Agent Rollout Distributions by Model Size

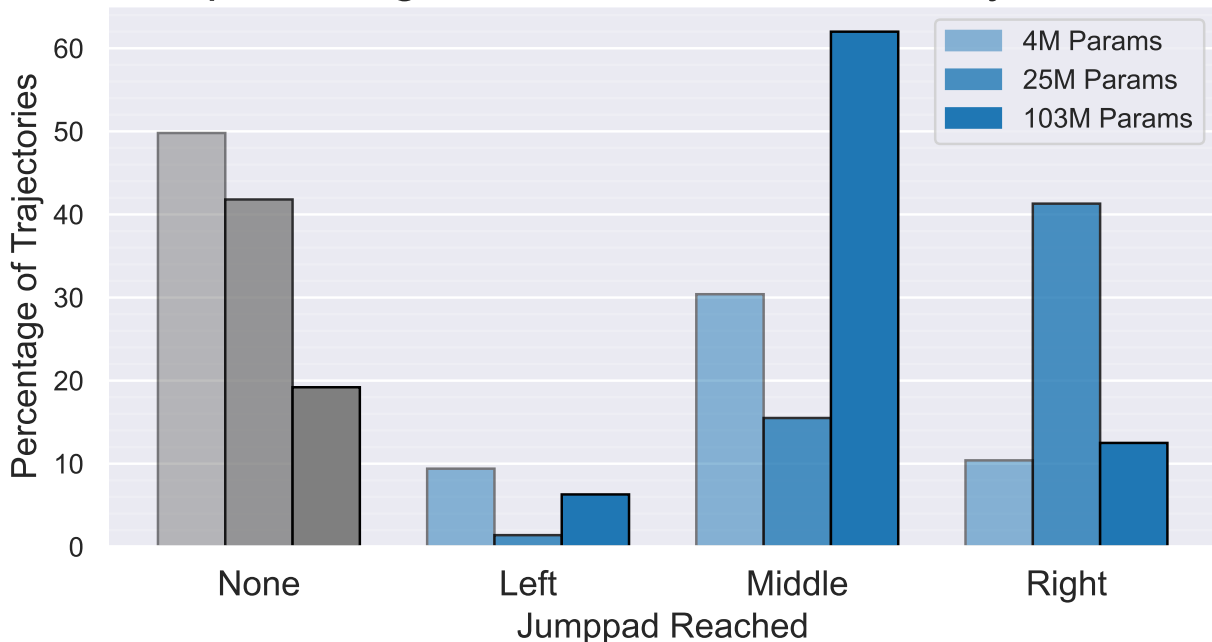


Figure 12. Distribution of jumppads reached by various size models (4M, 25M and 103M parameters) trained from scratch on the task-specific dataset used for fine-tuning the base model. Importantly, we see that task failure rates (the grey bars on the left) decrease as the number of parameters increases, even given the same size of dataset and number of training updates.

The jumppad distributions for these models are provided in Figure 12. We see that these smaller models have much greater failure rates than the larger 103M parameter models shown in Figure 5, demonstrating that larger models are beneficial for imitation learning from pixels even on this relatively small task-specific dataset of 300 trajectories. While larger models still may be beneficial (particularly with pre-training on our large unsupervised dataset described in Section 3.2), larger models would further increase the crucial inference cost and we find that 103M parameters is sufficient for further alignment, as demonstrated in Figure 5.

E.2. Preliminary Analysis of Model Alignment with Scale

To complete our ablation, we now investigate how pre-training and model size affects online alignment. To do so we followed the procedure in Appendix A to generated preferences as in Section 3.4. We then trained corresponding reward models and compare aligning these models trained from scratch to our pre-trained and fine-tuned model, as shown below in Figure 13.

Overall, the results are relatively high variance due to the small dataset these results are based on. For example, we see that our pre-trained model (brown) aligns significantly better than the equivalent size model trained from scratch (green) when

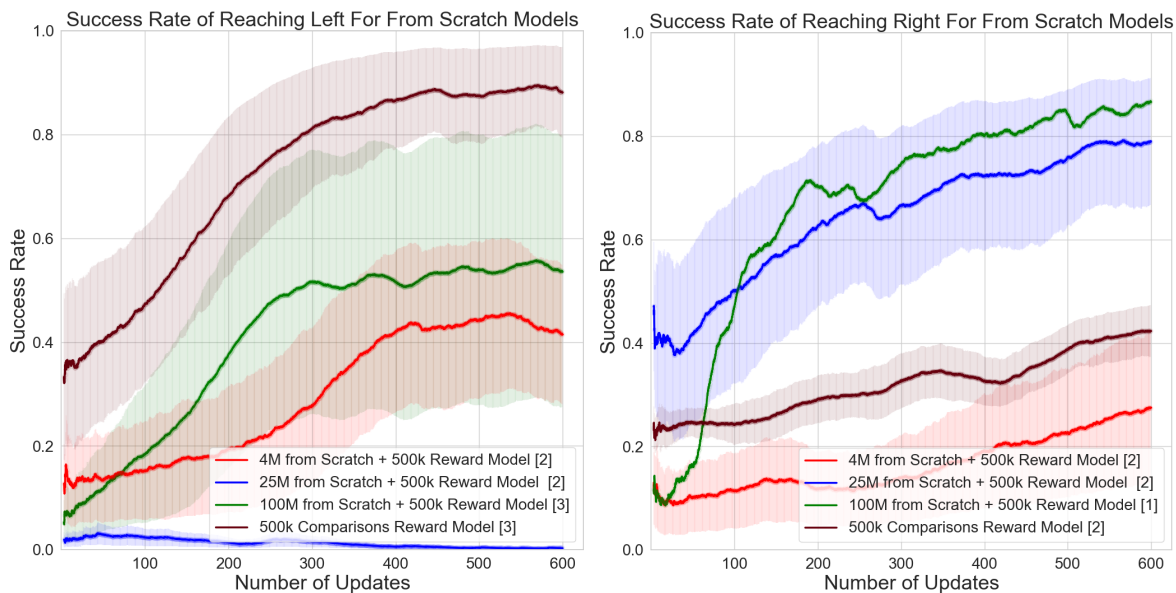


Figure 13. Left and right jump pad success rate during online alignment for models of different sizes trained from scratch using corresponding reward models trained on 500k comparisons.

aligned left, and worse when aligned right, but this is likely just due to the lack of diversity in the pre-trained+fine-tuned model as explained in Section 3.6.2. However, bearing that in mind, we can see some general trends emerging. In particular, we see some indications that larger models generally align better (ignoring the left-aligned 25M model and the right-aligned pre-trained 100M model due to the substantial left/right bias associated with these models) and allowing for differences in initial performance due to minor left/right bias, since the success rate generally increases more quickly during alignment as model size increases.

We also note that in this experiment we only considered using the original reward models trained on 500k comparisons, in order to see whether it was possible to successfully align a model trained solely on our small task-specific dataset. As noted in the previous section, these models have significantly less diversity in their behavior than the model first pre-trained and then fine-tuned. This makes it much more costly (in terms of human time) to generate sufficient labeled examples of the desired behavior to properly train the corresponding reward model (for example, less than 10% of trajectories reach the left jump pad for the model trained from scratch compared to over 30% for the pre-trained + fine-tuned model). This means that while these results show an upper bound in terms of reward model performance, we would expect the larger and pre-trained models to have less degradation in their alignment when using reward models trained on smaller quantities of preference data, and therefore for larger pre-trained models to perform even better in more practical settings.

F. Reward Model Performances by Jumpad

Test reward model performances against number of comparisons used for training by jumpad are shown below in Figure 14.

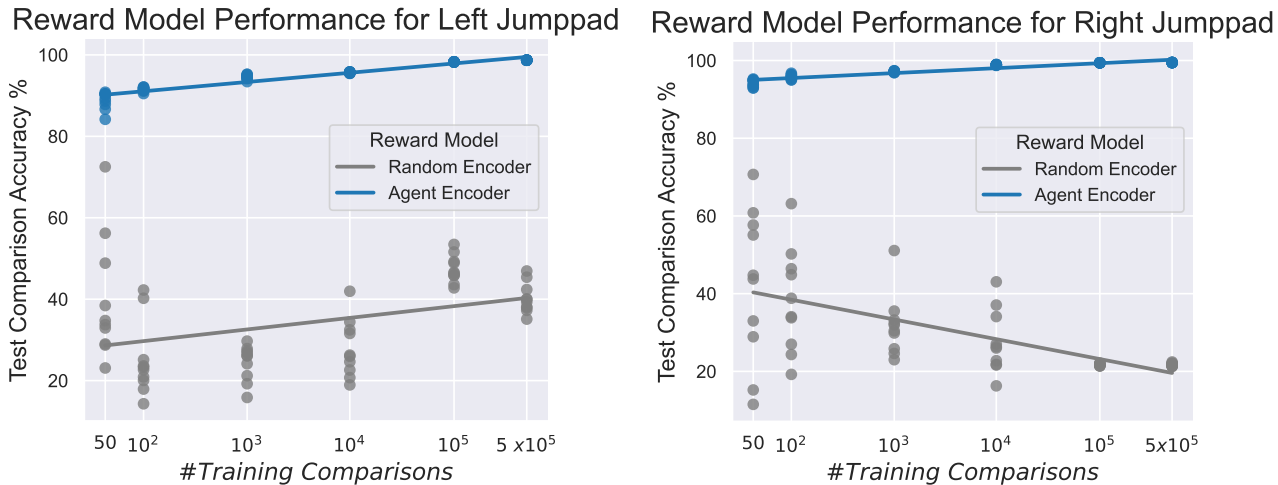


Figure 14. Test reward model performances against number of training comparisons by jumpad.

Both jumpads show the same trend for the agent encoder, reaching $\sim 90\%$ performance for 100 comparisons and 100% performance by 500k comparisons. The random encoder is high variance, but generally increases in performance with training comparisons for the left jumpad, while decreasing in performance for the right jumpad. This surprising trend for the right jumpad could be because the reward model begins to overfit to the imbalanced trajectories discussed in Section 3.6.2 and shown in Figure 15. In other words, the reward model misinterprets the preferences and instead learns to prefer shorter trajectories that begin at the bottom left spawn point (from which 84% of the successful right-going trajectories arise) leading to the $\sim 20\%$ accuracy that we see for higher numbers of comparisons. The agent encoder based reward model is better able to distinguish these trajectories and infer the true underlying preference that better fits the data.

G. Motivation for the Use of REINFORCE for Agent Alignment

Our proof-of-concept uses REINFORCE (Williams, 1992) for online alignment of our agent, as discussed in Section 3.6. While much of the RLHF literature uses PPO (Schulman et al., 2017), we note that recent work on LLMs has found PPO to be unnecessarily complex for RLHF (Ahmadian et al., 2024). This is due to the fact that in the standard RLHF framework, the reward is only provided at the end of the trajectory, meaning that we generally just want to reinforce entire trajectories rather than attempt credit assignment at each timestep using an advantage function, as is typically done with PPO. Additionally, Ahmadian et al. (2024) found that importance clipping rarely occurs in practice in RLHF, since the final aligned policy is kept close to the initial fine-tuned policy. This is reflected by the use of REINFORCE in recent state-of-the-art LLMs (Google Deepmind, 2024). As a result, we use REINFORCE for simplicity in our proof-of-concept, but note that more complex tasks or feedback mechanisms may warrant the additional complexity of more modern reinforcement algorithms such as PPO.

H. Investigation into Discrepancy in Aligning Agent to Reach Right Jump pad

H.1. Understanding Discrepancy between Left and Right Jump pad Trajectories

Since the task of aligning our agent left or right is seemingly equivalent, we would expect to be able to align the agent similarly. Surprisingly however, we found that our fine-tuned agent did not align as quickly towards the right jump pad as the left, only reaching around a $\sim 40\%$ success rate (in the absence of preference fine-tuning) after one day of training (as shown in Figure 9) compared to around $\sim 90\%$ for the left jump pad (as shown in Figure 8). In order to investigate this discrepancy, we analyzed the rollouts of the fine-tuned agent, shown in Figure 15.

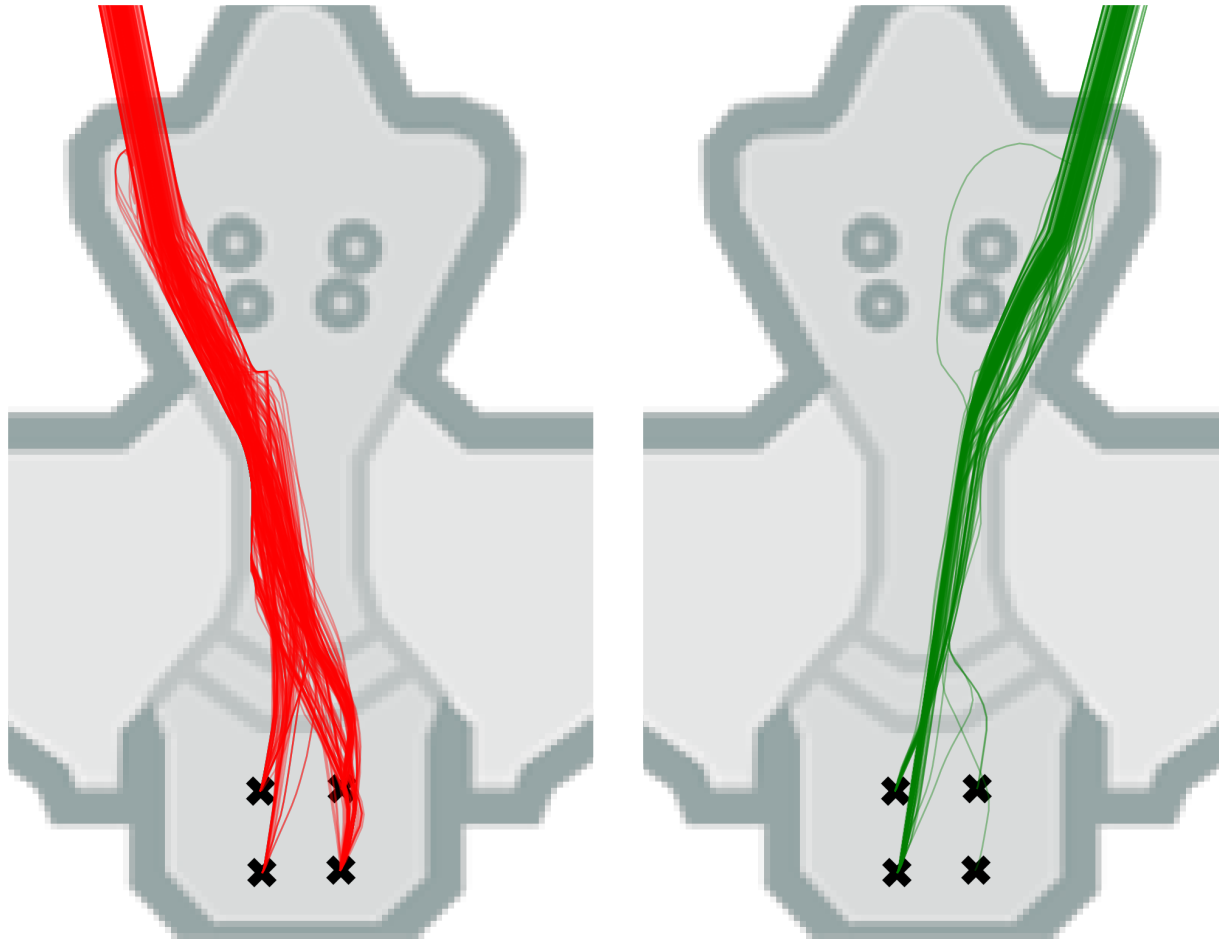


Figure 15. Fine-tuned agent trajectories which reached the left (red) or right (green) jump pads. While fine-tuning enables more efficient preference labelling, it reduces diversity, potentially limiting alignment.

We see that the trajectories that reach the left jump pad start relatively evenly from the 4 spawn locations. However, of the trajectories that successfully reach the right jump pad, only 1% originated from the spawns on the right hand side. Therefore it is unsurprising that it is more difficult for the agent to learn to go right, given that in half the episodes (from the right spawn locations) the agent rarely navigates to the right jump pad to receive reward to reinforce its behavior. To confirm this hypothesis, we instead attempt to align the base agent (before fine-tuning).

H.2. Alignment of Base Model for Comparison with Fine-Tuned Model

To understand how trajectory diversity affects alignment, we now consider aligning the base agent using the same reward models (trained on the fine-tuned agent). By plotting the successful trajectories that reach the left and right jump pads we see that the base agent (left) has a greater diversity than the fine-tuned agent (right). However, we note that the success rate for reaching the left and right jump pads is lower for the base model (as in Figures 3 and 4), so there are fewer trajectories.

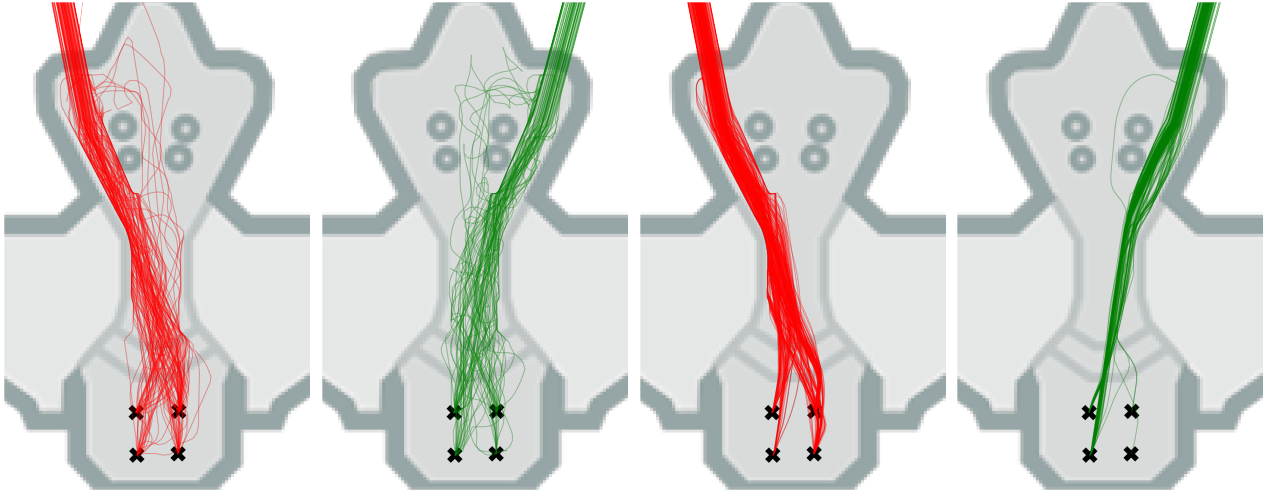


Figure 16. Base agent (left) and fine-tuned agent (right) trajectories for which the agents successfully reached the left (red) or right (green) jump pads. While fine-tuning provides a greater success rate, enabling more efficient preference labelling, it also reduces diversity of trajectories.

We now align the base agent to reach the left and right jump pads using the reward models trained on the fine-tuned agent, as shown below. We find that the agent can be aligned more symmetrically with both the left and the right jump pads, although alignment with the left jump pad still has a slightly better performance. However, in comparison to alignment of the fine-tuned agent (Figures 8 and 9), we see that the alignment is much slower, starting at a lower success rate, not increasing as quickly during training, and reaching a lower final success rate. As before, we see the same general trend that higher accuracy reward models (using more preference data) lead to better alignment.

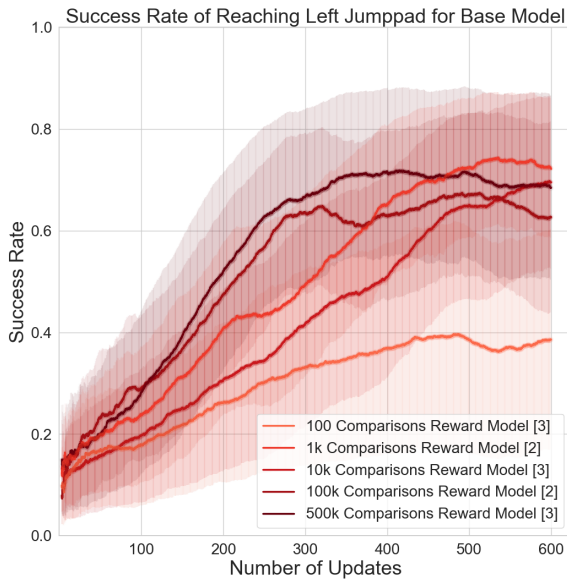


Figure 17. Left jump pad success rate for base agent using fine-tuned agent reward models.

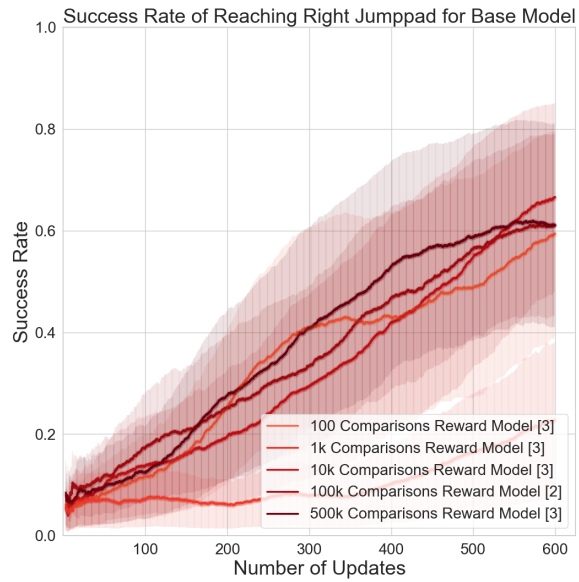


Figure 18. Right jump pad success rate for base agent using fine-tuned agent reward models

I. Final Aligned Agent Jump pad Distributions

Jump pad distributions for our final agents aligned to go left and right using preference fine-tuning and online alignment with reward models trained on 500k preferences are shown below.

First we partially align our agents with preference fine-tuning using our (500k comparison) reward models, so that the behaviour distributions are closer to the desired behaviour distributions to reduce the alignment required online, as shown in Figure 19.

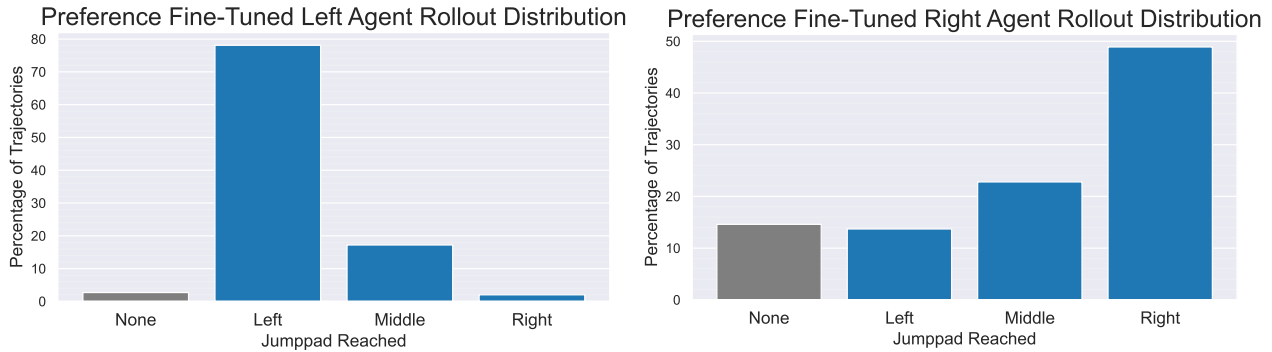


Figure 19. Left and right jump pad success rate for agents partially aligned with preference fine-tuning with reward models trained on 500k preferences.

We see that preference fine-tuning starts to align our agents towards the desired behaviour, but does not fully align our agents. Therefore we then perform online reinforcement learning using our (500k comparison) reward models until our agents are fully aligned.

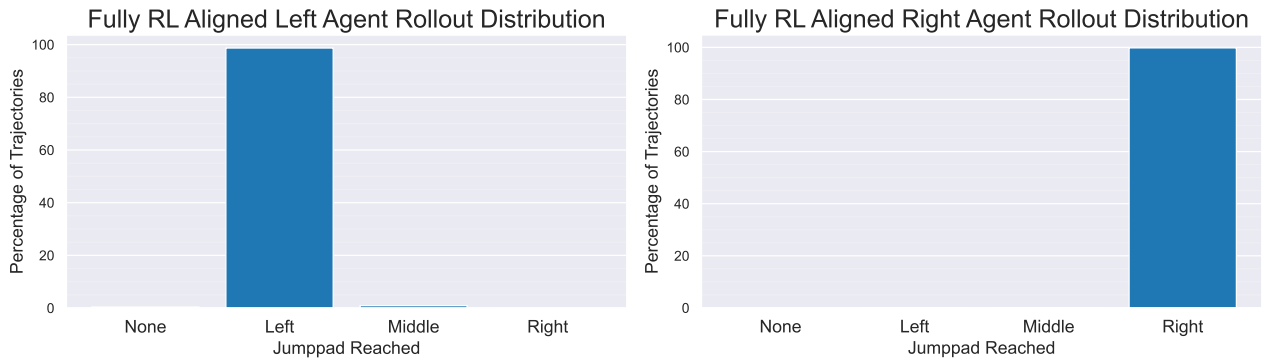


Figure 20. Left and right jump pad success rate for our fully aligned fine-tuned agents using preference fine-tuning and online reinforcement learning with reward models trained on 500k preferences.

Final evaluation shows that our agents have now been effectively fully aligned with our desired behaviour.

J. Limitations and Further Work

Our work provides a proof-of-concept of an approach for training embodied agents to act as desired in complex 3D environments. For this procedure to be applied in practice in video games and other domains such as robotics, the efficiency of this pipeline will be essential.

One limitation of our approach is that we assume access to a large amount of human data on the environment of interest to pre-train a base model. In practice however, when designing a game, large amounts of human data may not yet be available, and even for existing games it may not be possible to access. A potential solution may be to use a ‘gaming foundation model’ trained on similar games (with pixel input and action controller output). Equivalently in robotics, the collection of general cross-objective and embodiment datasets is becoming more important for training general robotic agents (Embodiment-Collaboration et al., 2024). We believe the potential transfer of models pre-trained across environments will be an exciting direction for future work.

Investigating developments in LLM architectures and pre-training could also be of interest for further work. For example, the context window used by the transformer H corresponds to the memory of the agent, so developments in increasing or augmenting the context window in LLMs such as Longformer attention (Beltagy et al., 2020) or Retrieval-Augmented Generation (RAG) (Lewis et al., 2021), could similarly be incorporated to increase the memory of agents trained with this approach, helping to address the issues with partial observability in complex 3D environments.

Another limitation of our proof-of-concept that we discuss in Section 3.4 is that we utilize synthetic preferences. While this may be a realistic option for many use cases, potentially using VLMs-as-a-judge (Zheng et al., 2023; Li et al., 2024), real human feedback may be required in general. As well as potentially introducing noise to the preference labels, this process can be costly in human time, especially for agents on modern console games which must often be run in real-time in order to be rendered. Therefore supervised fine-tuning on relevant behaviors to improve preference labeling efficiency could help to reduce this human time requirement. However, knowledge transfer from training LLMs could again be relevant here. Recent work on providing human feedback for LLMs has used a hybrid form of feedback that combines preference and evaluative feedback, in which responses are grouped into a batch of size N and simultaneously compared on a preference scale of size P , which enables larger numbers of comparisons to be extracted from a given number of responses, improving the time efficiency of providing feedback. For example, InstructGPT (Ouyang et al., 2022) uses $4 \leq N \leq 9$, $P = 7$ while Llama2 (Touvron et al., 2023) uses $N = 2$, $P = 4$. As N and P increase, more information can be extracted from the provided human feedback. For example, with $N = 5$, $P = 5$ and assuming no category duplication (no trajectories are considered equal), $\binom{5}{2} = 10$ comparisons can be extracted, which is equivalent to 2 bits of information per trajectory watched, compared to just 0.5 bits per trajectory for default pairwise comparisons with $N = 2$, $P = 2$. This results in a $4\times$ improvement in feedback efficiency for human labellers, at the cost of potential label noise due to the additional mental overhead required. Similar strategies could be applied to providing feedback to agents to make the process more time efficient.

A final limitation we consider in our proof-of-concept is the ability to run agents online, since embodied agents are much more challenging to run online than LLMs, even in the context of video games. For more complex behaviors and tasks this may become prohibitively expensive. Fortunately, developments in RLHF for language models can also be utilized here. We demonstrated in Section 3.6 that an initial step of preference fine-tuning, corresponding to Reinforced Self-Training (ReST) (Gulcehre et al., 2023) with a single iteration, can improve alignment efficiency. However, the full procedure using multiple iterations could be used to further improve the sample efficiency of aligning with preferences while maintaining the benefits of online exploration. Other recent work has investigated aligning models completely offline. Direct Preference Optimization (Rafailov et al., 2023) provides an approach for optimizing a model to align with preferences without the need for a reward model or online training, while (Hu et al., 2023) uses offline reinforcement learning with pre-generated samples and rewards. Additionally, efficient fine-tuning strategies such as LoRA (Hu et al., 2021) could be used to reduce the hardware requirements for the fine-tuning of a large base model for individual use-cases. These new approaches provide promising directions for further work in the context of agents to improve the efficiency or potentially even remove the need for online training completely. However, the extent to which active online learning is required for true generality is still an open question (Ostrovski et al., 2021) as we discuss in Appendix D.

In summary, we believe there is significant potential for transfer from recent developments in large language models to agents, that could help to address many long-standing limitations and open-problems for decision-making agents. We believe these will open up exciting new research directions in the coming years.